Institute of Applied Physics

Annual Report

2007

seit 1558

Friedrich-Schiller-Universität Jena

Publisher
Friedrich Schiller University Jena
Institute of Applied Physics
Max-Wien-Platz 1
D-07743 Jena
Germany

Authors
Prof. Dr. Andreas Tünnermann
Prof. Dr. Frank Wyrowski
Dr. Ernst-Bernhard Kley
Dr. Stefan Nolte
Dr. George Onishchukov
Dr. Jens-Peter Ruske
Dr. Holger Zellmer

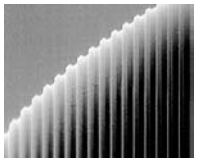

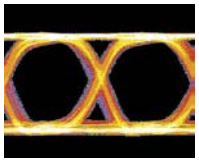

This annual report details the activities of the Institute of Applied Physics (IAP) of the Friedrich-Schiller-University Jena. It provides information on the people working at the IAP and contains a selection of scientific and technological achievements obtained by our scientists, engineers, and technicians.

In 2001 the IAP has further strengthen its core competences in the field of Optical Technologies by focussing the internal research resources. Research highlights in 2001 being the demonstration of an optical three dimensional coupler in glass manufactured by femtosecond-laser-machining, the efficient guiding of light in nanostructured low index materials, and the realization of a fiber amplifier system delivering output powers up to 100 W in ultrashort pulse operation.

Today, in these areas the IAP is on the road from research to revenue. The company Guided Color Technologies GmbH (private company limited by shares) was formed in 2001 by IAP-staff to transfer IAP-expertise on fiber lasers and integrated optical elements into products.

The research activities had been partially supported by the European Commission Directorate-General XII: Science Research and Development, German Ministry of Education and Research, German Research Foundation, Thuringian Ministry of Science, Research and Art and industrial clients with a budget of about 2 million €.

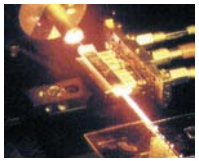

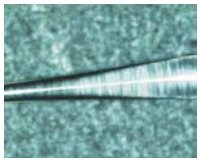

Looking back at the past year, in the name of the entire staff of the IAP I thank all those who supported our institute. Furthermore, thanks to our partners and customers among universities, research institutes and industry for excellent collaboration in various projects. This collaboration will be surely the key for further achievements.

My sincere thanks go to all IAP staff for their competent work,
and their commitment and willingness to face new challenges.
Due to their work, the IAP is well prepared for new tasks in future.

Jena, April 2002

Prof. Dr. Andreas Tünnermann
(Director of the Institute of Applied Physics)

The Institute of Applied Physics at the Friedrich Schiller University Jena has a longstanding tradition and competence in design, fabrication and application of active and passive photonic elements for both, optic and optoelectronic devices. A total staff of more than 30 scientists and engineers is presently working in education and R&D. In addition, about 20 diploma and PhD students and visiting scientists are researching at the IAP. Focal point of research is the generation, control and amplification of spatially and/or temporally confined light.

The institute has a floor space of 1,200 m^2 with installed clean rooms and optical laboratories including microstructure technology (electron beam and photo lithography, reactive ion and reactive ion beam etching, diffusion and ion exchange ovens, coating facilities, scanning electron and atomic force microscopy), optic/optelectronic testing and measuring instrumentation.

Research Profile

The Institute of Applied Physics at the Friedrich Schiller University Jena is engaged in the development of:

· Advanced micro-and nano-processing technology
· All solid state lasers
· Amplitude and phase masks
· Calibration tools
· Electro-optical materials
· Fiber and waveguide lasers and amplifiers
· Integrated optical devices
· Microoptics (refractive/diffractive)
· Nonlinear optical devices
· Physical optical elements
· Ultrafast optics

Staff Members

Abbe, Sylvia		
Augustin, Markus		
Bakonyi, Zoltán	Dr.	
Barthe, Guillaume		
Clausnitzer, Tina		
Cumme, Matthias		
Drauschke, Andreas		
Dubs, Carsten	Dr.	
Erdmann, Tobias		
Fuchs, Hans-Jörg	Dr.	
Gräf, Waltraud		
Gründer, Hans-Georg		
Grusemann, Ulrich		
Hartung, Holger		
Harzendorf, Torsten		
Häußler, Sieglinde		
Hoehl, Arne		
Höfer, Sven		
Jungebloud, Linn		
Kley, Ernst-Bernhard	Dr.	Microstructure Technology · Microoptics
Kling, Christoph		
Kölling, Kevin		
Liem, Andreas		
Limpert, Jens		
Lühr, Hendrik		Coordination office Optomatronik
Martin, Bodo		

Nolte, Stefan	Dr.	Ultrafast Optics
Onishchukov, George	Dr.	Optical Communication Systems
Otto, Christiane		
Riedel, Peter	Dr.	
Rockstroh, Sabine		Secretary
Rockstroh, Werner		
Ruske, Jens-Peter	Dr.	Integrated Optics
Schelle, Detlef		
Schmeißer, Volkmar		
Schmidt, Holger		
Schönke, Johannes		
Schnabel, Bernd	Dr.	
Schreiber, Thomas		
Steinberg, Carola		
Steppa, Denny		
Thieme, Mike		
Thomas, Jens		
Triebel, Peter		
Tünnermann, Andreas	Prof. Dr.	**Director of the Institute**
Werner, Ekkehard		
Will, Matthias		
Wittig, Lars-Christian		
Wolschendorf, Maik		
Wyrowski, Frank	Prof. Dr.	Optical Engineering
Zeitner, Brit		
Zellmer, Holger	Dr.	Fiber and Waveguide Lasers
Zöllner, Karsten		

Guest Scientists

Willert, Markus	Robert Bosch GmbH
Kluge, Michael	Schott Glas
Anders, Jens	Klinik für Orthopädie der FSU Waldkrankenhaus "Rudolf Elle" gGmbH
Müller, Stefan	Faseroptik Jena GmbH
Senthilkumaran, Paramasivam	Indian Institute of Technology, Guwahati, India
Flinn, Gregory	Toptica AG
Müller, Moritz	Osram OS
Wolf, Michael	Universität Mainz

Lectures

- **Summer Semester 2001**

Prof. Dr. Frank Wyrowski

Simulation und Design in der Optik	(Wahlvorlesung)
Simulation und Design in der Optik	(Wahlübungen)
Wellenoptisches Systemdesign	(Seminar)
Experimente im virtuellen Labor	(Praktikum)

Prof. Dr. Andreas Tünnermann

Experimentalphysik	(Vorlesung)
Physikalisches Grundpraktikum	(Praktikum)
Institutsseminar	(Seminar)

Prof. Dr. Andreas Tünnermann
Prof. Hartmut Bartelt

Mikrooptik und Integrierte Optik	(Wahlvorlesung)

Prof. Andreas Tünnermann
Dr. Holger Zellmer
Dr. Ernst-Bernhard Kley
Dr. Jens-Peter Ruske

Mikrooptik und Integrierte Optik	(Wahlpraktikum)

Dr. George Onishchukov
Prof. Dr. Andreas Tünnermann

Faseroptische Datenübertragungssysteme	(Wahlvorlesung)

Dr. Jens-Peter Ruske / Dr. Holger Zellmer

Experimentalphysik	(Seminar)

- **Winter Semester 2001/2002**

Prof. Dr. Frank Wyrowski

Simulation und Design in der Optik	(Wahlvorlesung)
Simulation und Design in der Optik	(Wahlseminar)
Wellenoptisches Systemdesign	(Wahlseminar)
Experimente im virtuellen Labor	(Wahlpraktikum)

Prof. Dr. Andreas Tünnermann

Grundlagen der Laserphysik	(Wahlvorlesung)
Erzeugung und Manipulation von geführtem Licht	(Wahlpraktikum)
Physikalisches Grundpraktikum	(Praktikum)
Institutsseminar	(Seminar)

Prof. Dr. Andreas Tünnermann
Prof. Hartmut Bartelt

Mikrooptik und Integrierte Optik	(Wahlvorlesung)

Prof. Andreas Tünnermann
Dr. Holger Zellmer
Dr. Jens-Peter Ruske

Aktive und passive Bauelemente geführter optischer Wellen	(Wahlvorlesung)

Dr. Jens-Peter Ruske
Dr. Holger Zellmer

Experimentalphysik	(Seminar)

Diploma Theses

Mike Thieme
Effiziente Holographie durch den Einsatz von Strahlformungselementen

Tina Clausnitzer
Das Potenzial der Nahfeldlithographie zur Herstellung von Gitterstrukturen

Tobias Erdmann
Proximity-Printing mit Phasenmasken,
ein neuer Ansatz in der analogen Photolithographie

Kevin Kölling
Aufbau und Erprobung eines Arbeitsplatzes
zur feldgestützten Domänenumkehr ferroelektrischer Kristalle

Danny Steppa
Aufbau und Erprobung eines Ultraviolett-Lasersystems
für die Mikroablation an optischen Oberflächen

Sven Höfer
Hochleistungsverstärkung eines schmalbandigen optischen Signals
in aktiven Lichtwellenleitern

Doctoral Theses

Zoltan Bakonyi
Nonlinear methods for spatial and temporal noise reduction
in ultrashort pulse optical systems (University of Szeged, Hungary)

Statistics

The research activities of the IAP in 2001 were partially supported by the European Commission Directorate-General XII: Science, Research and Development, German Ministry of Education and Research (BMBF), German Research Foundation (DFG), Thuringian Ministry of Science, Research and Art (TMWFK) and industrial clients with a budget of about 2 million €.

Total number of public funded projects: >20

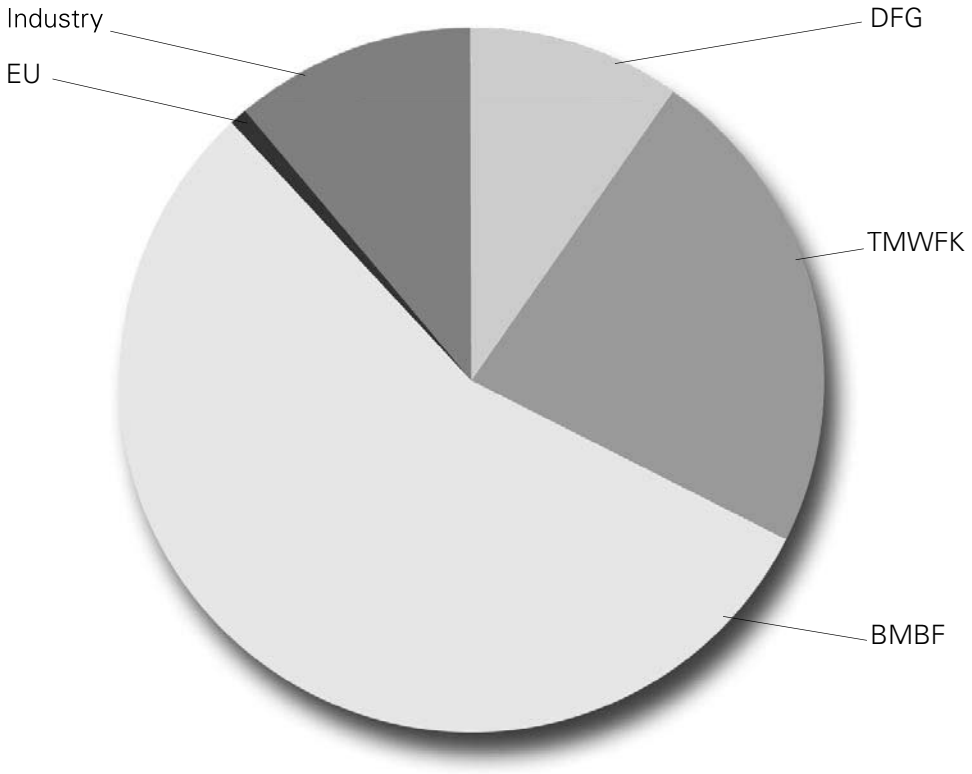

Externally Funded Projects

- **DFG Projects**

  Nanostrukturierte photonische Komponenten und deren Wechselwirkung mit Licht
  (Project term: 4/2000 – 3/2002)

  Teilchenstrahl-stimulierte Ultrapräzisions-Oberflächenbearbeitung;
  TP Ionenätzen
  (Project term: 1/2000 – 11/2001)

  Brechzahlmodifikation in optisch transparenten Materialien durch Strukturänderungen bei der Bestrahlung mit ultrakurzen Lichtpulsen; SFB TP B12
  (Project term: 1/1999 – 6/2002)

  Wellenoptisches Design monofunktionaler optischer Systeme
  (Project term: 8/2000 – 7/2002)

- **TMWFK Projects**

  Härtung und Strukturierung von Polymerschichten mit blauemittierenden Lasern
  (Project term: 10/1999 – 12/2001)

  Intra-Netz Optomatronik
  (Project term: 1/2000 – 12/2001)

  Integriert-optische Systemtechnik: Herstellung und hybride Integration
  von aktiven und passiven miniaturisierten optischen Elementen
  (Project term: 4/1999 – 3/2002)

  Integriert-optische Systemtechnik: Herstellung und hybride Integration von aktiven und passiven miniaturisierten optischen Elementen – Investitionen
  (Project term: 3/1999 – 12/2001)

Digitale Modulationskonzepte für Fotoprintingsysteme
(Project term: 3/2001 – 2/2003)

- **BMBF Projects**

  Herstellung strukturierter Beleuchtungskomponenten für die EUV-Lithografie
  (Project term: 5/2000 – 7/2001)

  Herstellung und Anwendung von Polarisationsgittern – SENTEX
  (Project term: 1/2000 – 3/2002)

  Diffraktive Kombinations-Optiken für Hochleistungsdiodenlaser
  (Project term: 10/1999 – 12/2003)

  Funktionale optische Komponenten mittels Nano-Replikationsverfahren (FOKEN)
  – Teilvorhaben: Prägewerkzeuge mit Schwerpunkt auf hohe Aspektverhältnisse
  (Project term: 9/2001 – 8/2003)

  MICROPHOT – Laserdirect: Faseroptische Hochleistungslaser für die Druckvorstufe
  – Teilvorhaben: Neuartige Skalierungskonzepte für Faserlaser und –verstärker in kontinuierlichem und gepulstem Betrieb
  (Project term: 7/2000 – 6/2003)

  MICROPHOT – OMP: Integriert-optische Modulationskonzepte
  im sichtbaren Spektralbereich
  (Project term: 7/2000 – 7/2003)

  Verbundprojekt Kompetenznetze Optische Technologien (Phase 2)
  im Teilvorhaben: Kompetenznetz OptoNet e. V.
  (Project term: 11/2000 – 2/2001)

Grundlegende Untersuchungen zur Materialbearbeitung sowie die Berechnung und Erprobung optischer Elemente zur Strahlformung ultrakurzer Laserpulse (PRIMUS)
(Project term: 5/2000 – 10/2002)

Laserstrahlformung mit Hilfe spezieller optischer Elemente
(Project term: 5/2000 – 10/2002)

German-Israeli Cooperation in Ultrafast Laser Technologies (GILCULT)
– Teilvorhaben: Ultrashort-pulse lasers and amplifiers
based on diode pumped fiber laser crystals
(Project term: 3/2001 – 2/2004)

Präzise Materialbearbeitung mit Ultrakurzpuls-Strahlquellen
– Teilvorhaben: Kurzpuls-Faserlaser CPA-System
(Project term: 7/2001 – 9/2003)

- **EU Projects**

  Development of New Dielectric and Optical materials and process-technologies for low cost electrical and/or optical packaging and testing of precompetitive Demonstrators – DONDODEM, BriteEuram
  (Project term: 9/1998 – 12/2001)

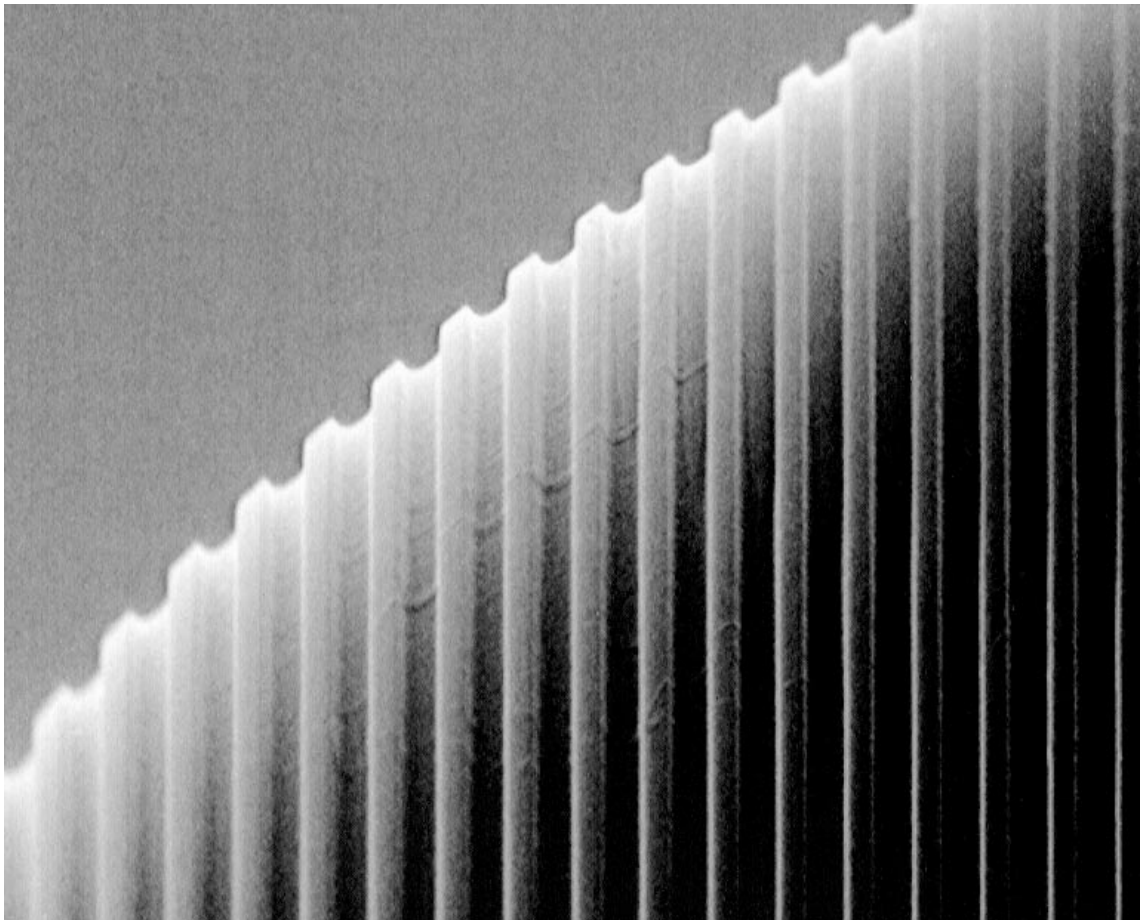

MICROSTRUCTURE TECHNOLOGY · MICROOPTICS

Achievements and Results

- Thick refractive beam shaping elements applied to laser diodes

Dr. Ernst-Bernhard Kley

In special beam shaping applications, a very high conversion efficiency and signal quality is needed. In such cases we prefer refractive beam shaping elements because of their excellent optical properties. A disadvantage of refractive elements is, that their profile depth depends on the beam diameter and the deflection angle, which we need to achieve the desired intensity distribution. It is easy to see that the profile depth of a refractive beam shaping element increases when the angular spectrum or the beam diameter are increased.

For the fabrication of refractive beam shaping elements, we usually employ gray tone lithography, which is a suitable technology to produce continuous three-dimensional profiles. One of the limitations of this technology is, that increased profile depth leads to proportional increased profile errors, higher aberrations and surface roughness. Apart from the difficulty to fabricate deep profiles with high accuracy and quality, we meet another problem: large profile depths combining large angles of profiles and non-paraxial incident waves may lead to spherical aberrations. In this case it is necessary to use special design methods which consider these effects.

We want to present a special beam shaping task for an application in safety engineering, in which beam shaping elements with profile depths up to 60 µm are used. We will show the design and fabrication process as well as discuss the reachable accuracy of the transformed signal. The optical setup is shown in Figure 1a. A wave coming from a laser diode has to be transformed into a line of constant intensity with a very high efficiency. An essential demand on the shown beam shaping setup is, to realize this transformation with only one element to avoid alignment problems. Parameters of the used laser diode beam were determined by measuring the intensity distribution along the fast and the slow axis at several distances from the laser diode. Figure 1b shows intensity distributions as well as fitted Gaussian functions at the element

plane. The distance between the waist of the laser diode beam and the beam shaping element, that determines the beam diameter, was chosen in order to minimize the profile depth of the element. Resolution limit given by the diffraction and the alignment conditions was considered. The following beam shaping parameters were used:

Illumination wave		Signal	
wavelength :	670 nm	distance from element :	140 mm
beam diameter (1/e²) :	1140 µm (fast axis)	line width (1/e²) :	0.7 mm
	320 µm (slow axis)	line length :	100 mm
numerical aperture :	0.31 (fast axis)		
	0.11 (slow axis)		
distance from waist :	1.2 mm		

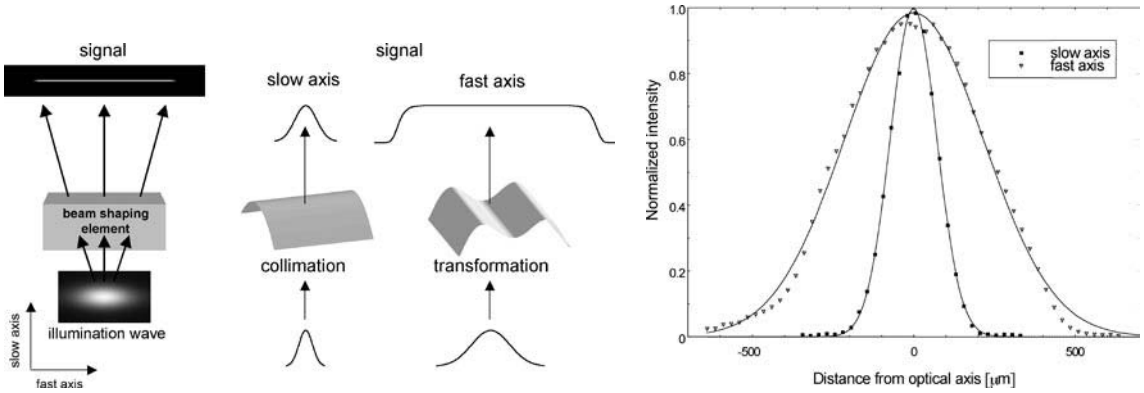

Figure 1 **a)** Optical setup of the present beam shaping task.
b) Line scans along the fast axis and the slow axis of the laser diode beam at the element plane.

As shown in Figure 1a, we can separate the beam shaping job into two tasks: in direction of slow axis we have to concentrate the intensity of the incoming wave, while in direction of fast axis we have to redistribute the intensity. This means, that in direction of slow axis we have to apply a cylindrical lens. In direction of fast axis we have to apply a beam shaping element, that transforms a Gaussian into a top hat intensity distribution. Beam shaping elements of this kind can be calculated analytically using design methods of geometrical optics, if the desired intensity distribution is a super-gaussian distribution of order n [6]. In this work, we calculated a beam shaping element using an order of n=20. The combination of both phases (cylindrical and beam shaping phase) and its unwrapping led to the surface profile shown in figure 2a, that was cut at a profile height of 41 µm.

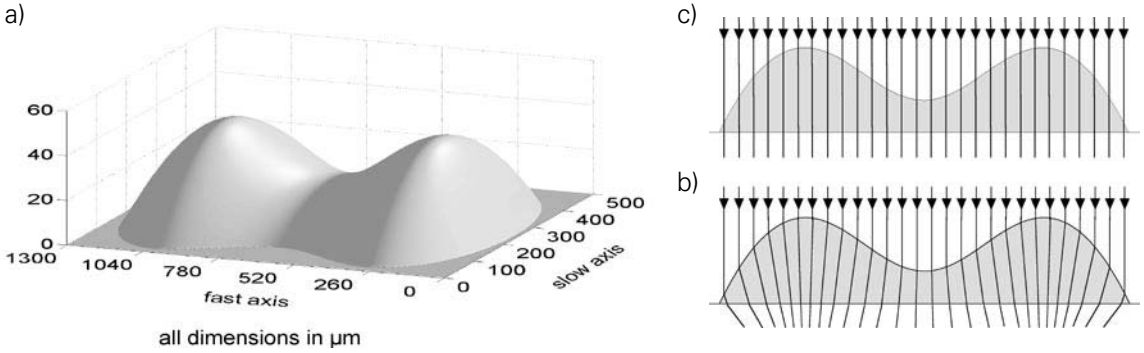

Figure 2 **a)** Surface profile of a designed beam shaping element, cut at a profile height of 41 µm.
b) Assumed way of light rays through the element using the Thin Element Approximation (TEA),
c) by using the Local Plane Interface Approximation (LPIA).

Lateral dimensions of the presented element are 1.3 mm (fast axis) and 0.5 mm (slow axis) to collect more then 99% of the incident light. As mentioned above, to fabricate thick refractive profiles, we have to consider effects that are caused by refraction of the incident wave at the element surface. The simplest way to describe the phase change of a wave which propagates through an optical element is to use the Thin Element Approximation (TEA). By using TEA we

assume, that the phase change $\varphi(x,y)$ depends only on the element height h(x,y) and it takes place in an infinite thin plane. This means, that if we would split an incident wave into several rays, they would propagate straight through the element, the phase change at every point of exit will be $\varphi[h(x,y)]$ (see figure 2b). TEA also leads to the easy calculation of the element profile for a given phase $\varphi(x,y)$ by

$$h(x,y) = \frac{\varphi(x,y)}{2\pi} \cdot \frac{\lambda}{n-1}$$

where λ is the wavelength and n is the refractive index of the element. For the validity of TEA we have to guarantee a few essential conditions. For example, the following relation has to be fulfilled if we use TEA to describe gratings:

$$x_{min} \cdot n \geq a \cdot \lambda$$

where x_{min} is the minimum feature size and a is a constant factor. This rule can be translated into a limit to the maximum rim angle α_{max} that can be accepted to use refractive structures. The maximum rim angle of the profile shown in Figure 2a has a value of 17 deg, but in our case ($n_{Element}$=1.62, λ=670 nm) α_{max} has to be less than 10 deg. In that case, an approximation by TEA does not allow us an acceptable accuracy. To check this fact, we calculated the optical effect of the designed element using the Local Plane Interface Approximation (LPIA) described in. With LPIA, we were able to calculate the phase function of an optical element under consideration of the refraction of the incident wave, its deflection and the resulting optical path (see Figure 2c). After calculating the phase and amplitude distribution behind the element by LPIA, we simulated the wave propagation to the signal plane with the spectrum of plane waves representation as propagation operator. The calculated intensity distribution is shown in figure 3.

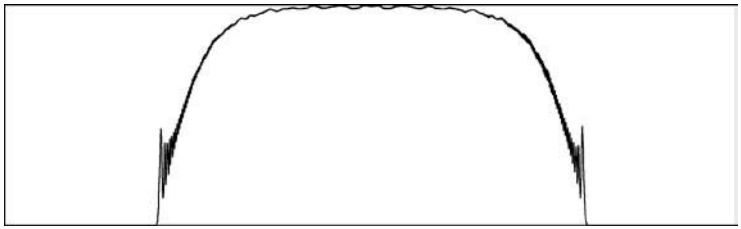

Figure 3 Simulated intensity distribution of the signal using LPIA.

The fabrication of the designed beam shaping element was done using gray tone lithography. We used HEBS-glass (high energy beam sensitive glass, Canyon Materials Inc.) as a mask blank and AZ 4562 photo resist. Using gray tone lithography, a profile error of 1–2% is reachable, in special cases it can go down to 0.2% of the total profile depth. The profile error can be splitted into profile aberration and profile roughness.

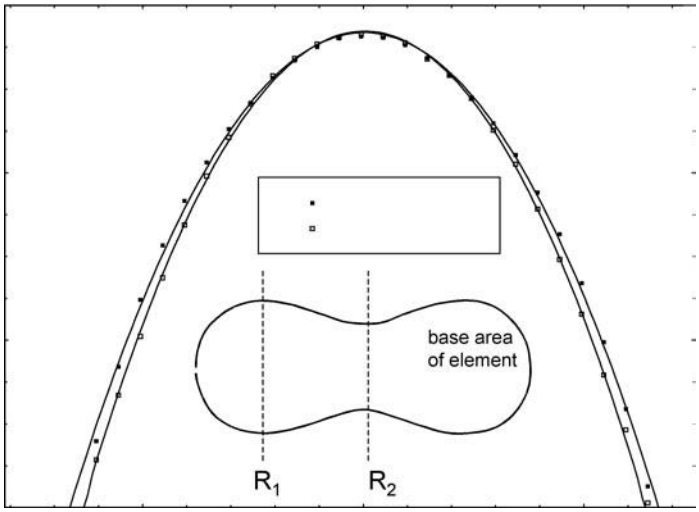

Figure 4 Measured profiles along the direction of slow axis of a fabricated element that cross the top (R_1) and the saddle point (R_2).

Profile aberrations are caused primarily by effects of the UV-exposure and development of the photo resist. Because of the fact, that the development occurs in both vertical direction and horizontal direction, different results can be found for equal desired profiles designed using various sags. For example, this effect leads to radius variation of the cylindrical profile that we apply to focus the slow axis (see section 3). Measured profiles along the slow axis direction of a fabricated element at the top (R_1) and the saddle point (R_2) are shown in Figure 4. The measurement was done using a confocal microscope. The measured curves were normalized in order to have the same maximum value. By fitting square functions on the measured profiles we calculated, that the profile radii differ by 9.2%.

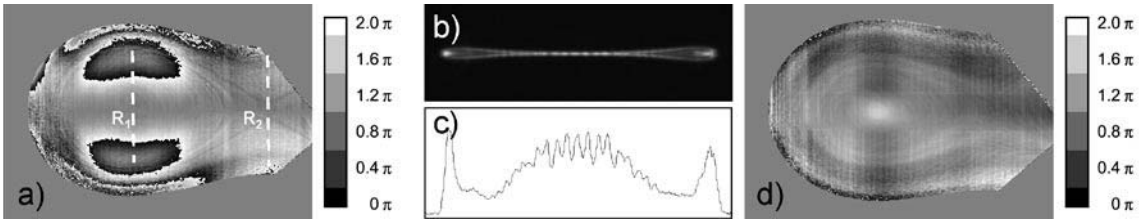

Figure 5 **a)** Phase difference of the left part of the fabricated element, calculated from the measured surface profile. **b)** Measurement of the realized intensity distribution. **c)** Line-scan of the distribution shown in b). **d)** Phase difference after correction of the element.

To find the profile aberration of the fabricated element, the measured surface profile was converted into the resulting phase profile. The designed phase was subtracted from this phase profile; the difference for the left part of the element is shown in Figure 5a by using the mod(2π)-representation. The dashed lines represent the profile scans (see Figure 4). The maximum phase aberration that is shown in figure 5a was measured to be about 2.3π. Additionally, in the presented distribution two areas can be seen that provide a lens function. Figure 5b shows the measured intensity distribution, generated by the fabricated element. The end of the measured distribution, which looks like an eye of a needle, is caused by the lens-like phase aberrations of the element. A line-scan of the measured distribution is shown in figure 5c. It is easy to see,

that the quality of the signal has to be improved. One opportunity to produce thick profiles with a better accuracy is to use iterations in the fabrication process. Therefore the measured, uncorrected profile of the fabricated element was used to calculate a correlation between the exposed electron dose and the profile height, which was adapted to the special profile shape we need. The profile aberration is shown in Figure 5d for an element fabricated using the correction, represented by the resulting phase difference. After the correction, the maximum phase aberration did not exceed 0.8π over the entire region, where the amplitude of the illuminating wave was higher than 5% of the maximum amplitude.

As mentioned above, not only the profile aberrations, but also the profile roughness impacts the signal quality. The profile roughness is caused by an effect of the electron beam writing and by inhomogenities in the photo resist film. Figure 6a shows the surface of the corrected element with a periodic structure, caused by electron beam writing effects; figure 6b shows a line scan of the same part. Such periodic structures lead to periodic intensity modulations that can be seen in the center of intensity line scan (figure 5c). Tempering the fabricated element in such a way, that only the surface was melted in order to preserve the global resist structure, we were able to smooth the surface and to decrease the surface roughness from 40 nm rms to 2 nm rms within the measured area (see Figure 6c).

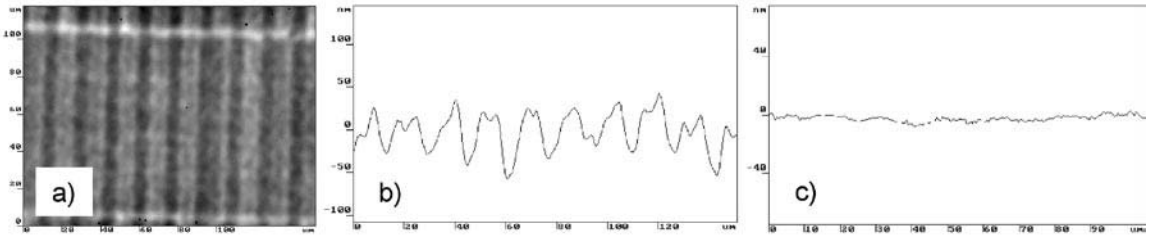

Figure 6 **a)** Surface of a fabricated element which shows a profile roughness caused by effects of electron beam writing. **b)** Line scan of structure shown in a). **c)** Profile roughness after smoothing.

An element was fabricated using the corrected correlation between electron dose and resulting profile depth. It was applied in the beam shaping setup. The produced intensity distribution was measured using a CCD-camera. Compared to the distribution shown in figure 5b, an improvement can be seen in figure 7a. However, endpoints of the line show significant widening. A possible reason to the widening is, that the diameter of the laser diode beam is too large in direction of fast axis, leading to diffraction effects at the border of the element. Figure 7b shows the intensity distribution of the unshaped beam at the same distance from the laser diode as the measured line. The intensity profile of the measured line is shown in figure 7c. Points of the curve represent maximum intensity at every cross section perpendicular to the line. The profile shows the same intensity modulations as the center of the line scan in figure 5c which is caused by the surface roughness of the element. The rms-value of the line intensity was 6.8%, the peak to valley deviation was measured to be 30%. After smoothing the surface profile, the homogeneity of the transformed intensity distribution was improved, see figure 7d. The rms was lower than 3.3%, the peak to valley deviation was 13%, the measured conversion efficiency was better than 90%.

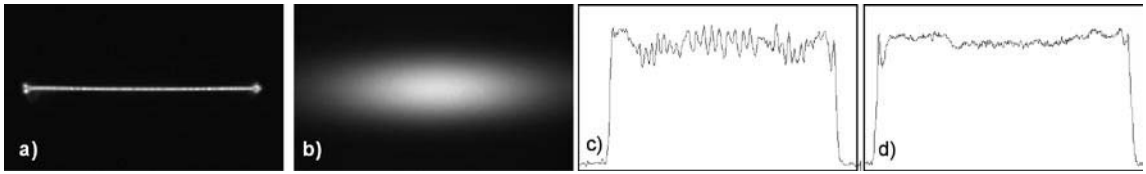

Figure 7 **a)** Resulting intensity distribution using a profile correction.
b) Intensity distribution of the unshaped beam at the same plane.
c) Scan of the line intensity before smoothing of the profile.
d) Scan of the intensity after smoothing of the element profile.

Investigations to further increase the performance of the elements are presently under progress in collaboration with industrial partners. The basic investigations had been partially funded by the DFG.

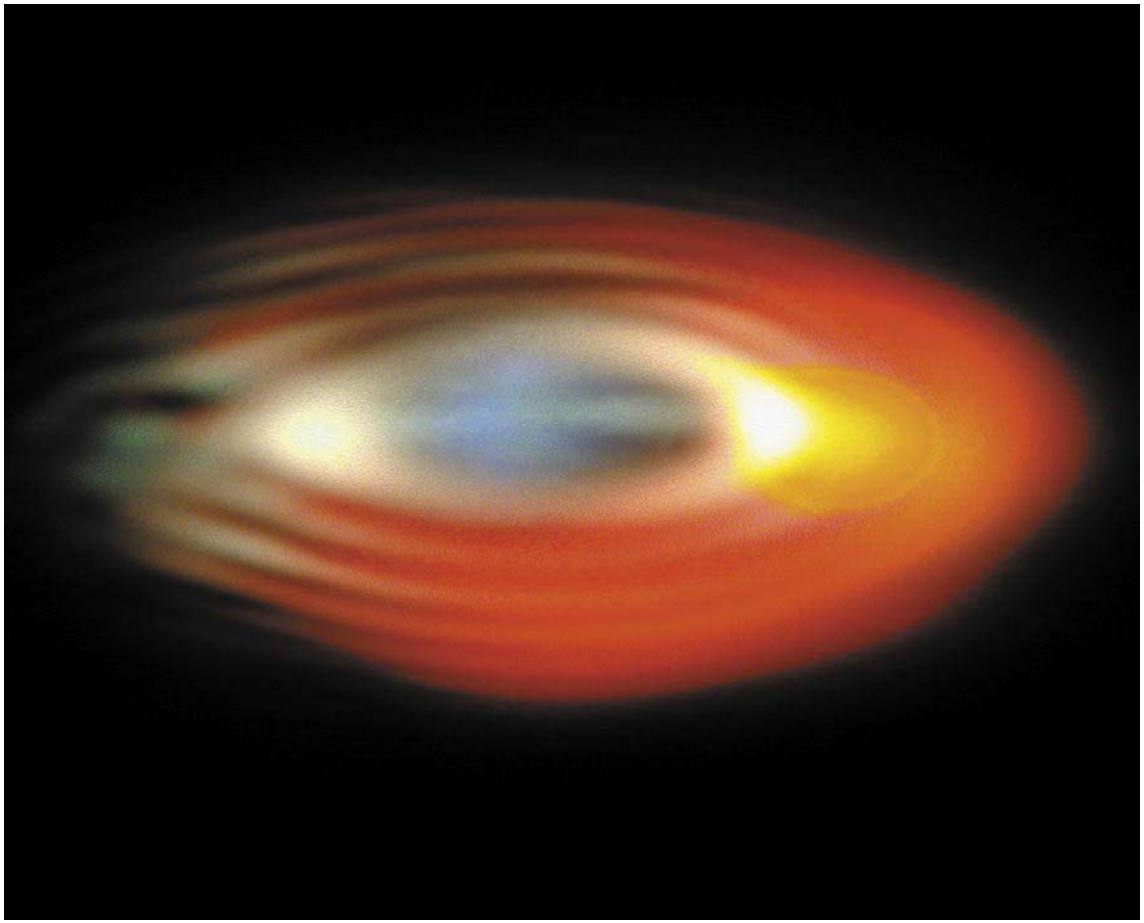

ULTRAFAST OPTICS

- Low loss integrated optical device fabrication in glasses by femtosecond laser pulses

Dr. Stefan Nolte

In the Ultrafast Optics group the interaction of high intensity ultrashort laser pulses with solids is studied. Besides precise micromachining the focus of our research is on the internal modification of transparent materials.

In 1996 it was discovered that a localized refractive index increase in transparent glasses can be achieved by focusing ultrashort laser pulses inside the material. By moving the sample with respect to the laser beam a refractive index profile can be generated that allows guiding of light as required for applications in Integrated Optics.

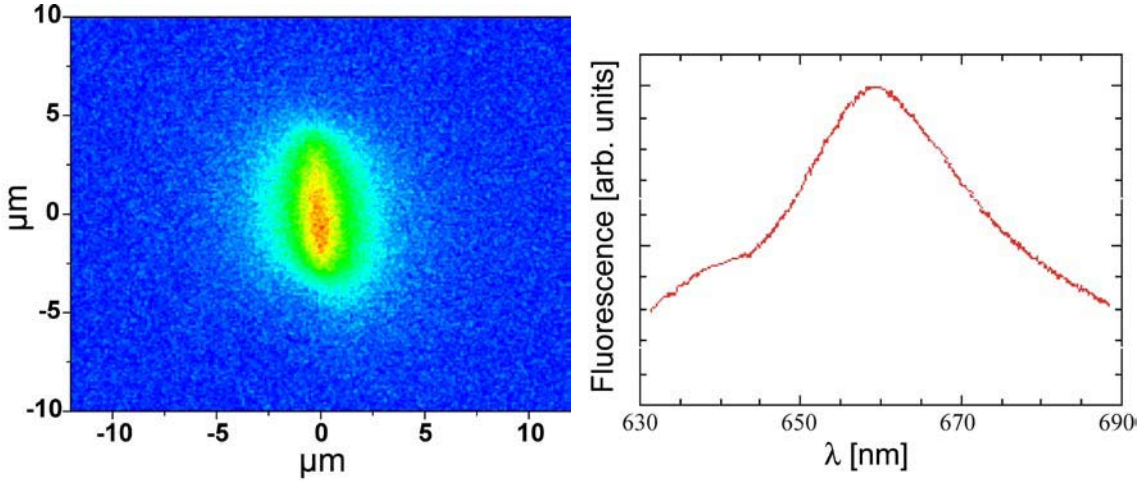

Figure 1 Density distribution of color centers across a waveguide written with femtosecond laser pulses in fused silica (left). Using a laser scanning microscope the color centers were excited and their flourescence detected. On the right the fluorescence spectrum of the color centers excited at 594 nm is shown.

During the past year we significantly improved the fabrication of integrated optics devices in different glasses by focused femtosecond (fs) laser pulses. In particular, we investigated the role of color centers for the refractive index changes. Although it was well-known that color centers are formed during the interaction of the femtosecond laser pulses with a dielectric, their role for the refractive index changes was unclear. Figure 1a shows the distribution of color centers across the end-surface of a fs-laserwritten waveguide in fused silica. The color centers were excited using a laser scanning microscope (LSM) at a wavelength of 633 nm and their fluorescence was detected. The density distribution follows the geometry of the laser beam focus (the femtosecond pulses were focused from the top using a 20x, 0.45 NA microscope objective). In Figure 1b the fluorescence spectrum of the color centers excited at 594 nm is shown.

While these color centers are formed during the waveguide writing process, they do not seem to be responsible for the refractive index modifications and the waveguiding properties. This can be concluded from the fact that the color centers can be annealed at 400°C. After this annealing process no fluorescence emission is observable anymore. In contrast, the waveguiding properties are preserved even when the sample is heated up to 500°C for several hours.

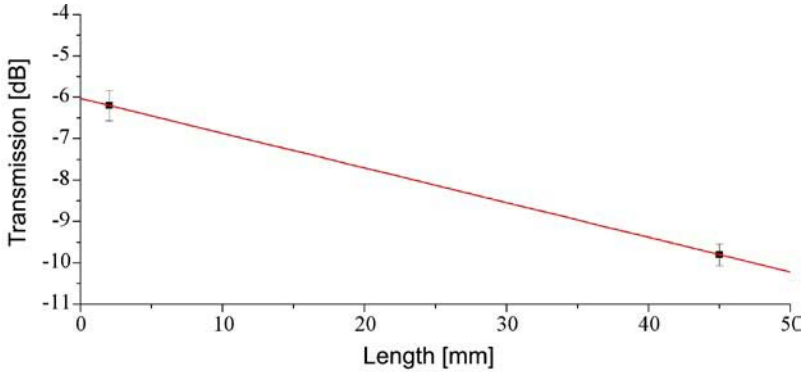

Figure 2 Transmission through a femtosecond written waveguide in fused silica. By using the cut-back method a damping loss of 0.8 dB/cm has been determined.

In order to be competitive with standard integrated optical waveguides it is important to write waveguides with low losses. Figure 2 shows the transmission losses of a waveguide in fused silica as a function of the waveguide length. We determined the damping losses using the so-called cut-back method. Therefore, a 4.5 cm long waveguide has been fabricated by moving a fused silica sample transversal to the focused laser beam. Both end-faces have been polished and the transmission of 514 nm laser radiation, that was coupled into the waveguide from a single mode fiber with NA = 0.11 (mode field diameter 3–4 µm), has been measured. Then a thin piece (thickness ~ 3 mm) of the sample was cut, the surface was polished again and the transmission through this short waveguide was determined. From the transmission values shown in Figure 2 a damping loss of 0.8 dB/cm can be deduced. However, the coupling efficiency of only 25% (-6 dB) is rather poor. This low coupling efficiency is mainly due to the mismatch in numerical aperture between the waveguide and the fiber used for coupling the laser radiation into the waveguide. By using a low NA fiber, we have been able to measure overall transmission losses of 3.5 dB in a femtosecond written waveguide of 4.5 cm length including coupling losses. This means that the damping must be significantly lower than 3.5 dB/4.5 cm = 0.78 dB/cm, since this value still includes the coupling losses.

Figure 3 Near-field distribution @ 800 nm at the exit of a symmetrical Y-splitter produced by ultrashort laser pulses. The two arms are split by 80 µm over a length of 1 mm.

Based on these promising values for the damping losses (which are the lowest values reported for fs-written waveguides so far) one can now turn to the fabrication of more complex structures. As an example Figure 3 shows the near-field distribution at the exit of a symmetrical Y-splitter. This device was produced by focusing 100 fs, ~ 1 µJ pulses of a Ti:sapphire laser system, operating at 800 nm at a repetition rate of 1 kHz, with a 10 x microscope objective (NA 0.25) into the bulk sample. The two arms of the splitter are divided by 80 µm, split over a length of 1 cm. This is equivalent to a splitting angle of approximately 0.5°. As is well-known, the maximum splitting angle is determined mainly by the refractive index difference between the bulk substrate and the waveguiding structure. Based on BPM (beam propagation method) simulations, we have shown that the two arms can be split by more than 300 µm when a refractive index difference of $3x10^{-3}$ is realized. Such a large splitting allows coupling to standard fibers.

Figure 4 Near-field distribution at the end of a three-dimensional splitter for a wavelength of 800 nm. The exits, which are not in the same plane as the entrance arm, are separated by ~ 40 µm. On the right a polarisation contrast microscope image of the device is shown (stretched in the vertical direction).

Although, such a Y-splitter demonstrates that the femtosecond direct writing technique is capable of producing planar devices, it does not reveal one of the main advantage of this technique, the possibility to write real three-dimensional photonic structures. Figure 4 shows the near-field distribution of light guided in the first three-dimensional integrated optical device fabricated by femtosecond laser pulses, a three-dimensional 1 x 3 splitter. In this case, none of the three

arms is in the same plane as the entrance arm of the splitter. The exits are separated by ~ 40 µm and the total device length amounts to 25 mm. Compared to a straight waveguide, this 3D-splitter shows additional losses of only 3 dB.

In addition to the possibility of writing three-dimensional photonic structures, the femtosecond direct writing method has the advantage that it is not restricted to special materials to which, e.g., the ion exchange process is adapted. Since the mechanism that creates the refractive index increase is quite universal waveguides can be written in practically all transparent materials using ultrashort laser pulses. This includes doped glasses, which allows to fabricate amplifying structures. Up to now, we have written waveguides in phosphate and silicate glasses doped with Er-, Yb- and Nd-Ions (see Figure 5). In a 3.2 cm long waveguide in Nd-doped glass we were able to measure amplification of 1.3 dB.

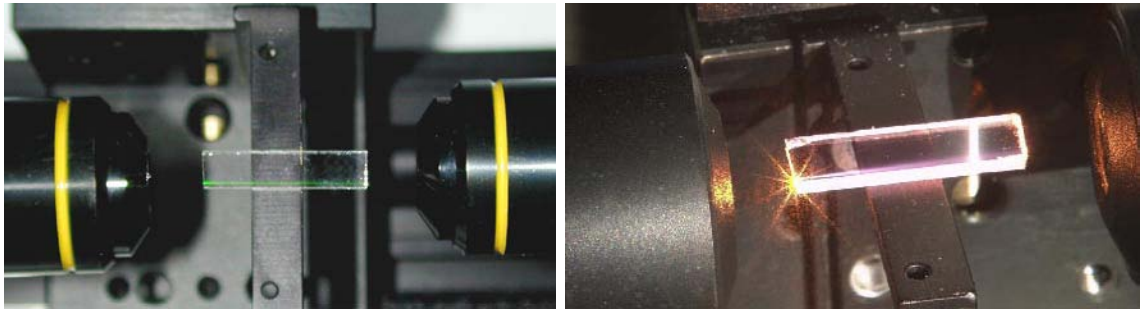

Figure 5 Waveguides in Er-/Yb-doped (left) and Nd-doped (right) silicate glasses.

Based on our know-how, we will extend our investigations to crystalline materials like $LiNbO_3$ to create integrated optical frequency doubling elements and modulators. In addition we are planning to build amplifying elements in doped materials.

The investigations had been partially funded by the DFG in the SFB 196.

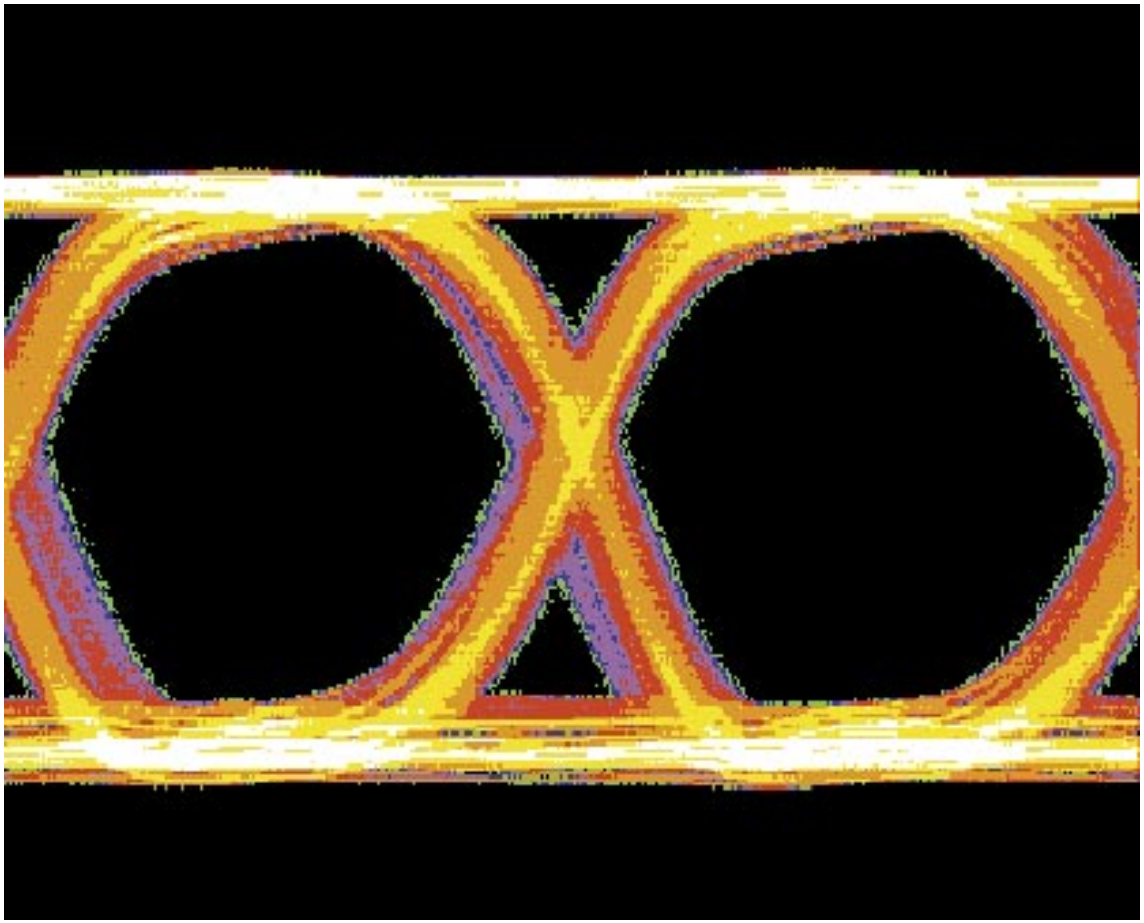

OPTICAL COMMUNICATION SYSTEMS

- High bit-rate optical fiber communication systems

Dr. George Onishchukov

The research in the field of optical fiber communication systems at the IAP is focused on the performance of high bit-rate systems based on soliton transmission. The emphasis is placed on the study of physical effects, which limit the transmission distance, using a re-circulating fiber loop set up (fig.1). During the past year, we have concentrated on the specific features of the system with in-line semiconductor optical amplifiers and saturable absorbers.

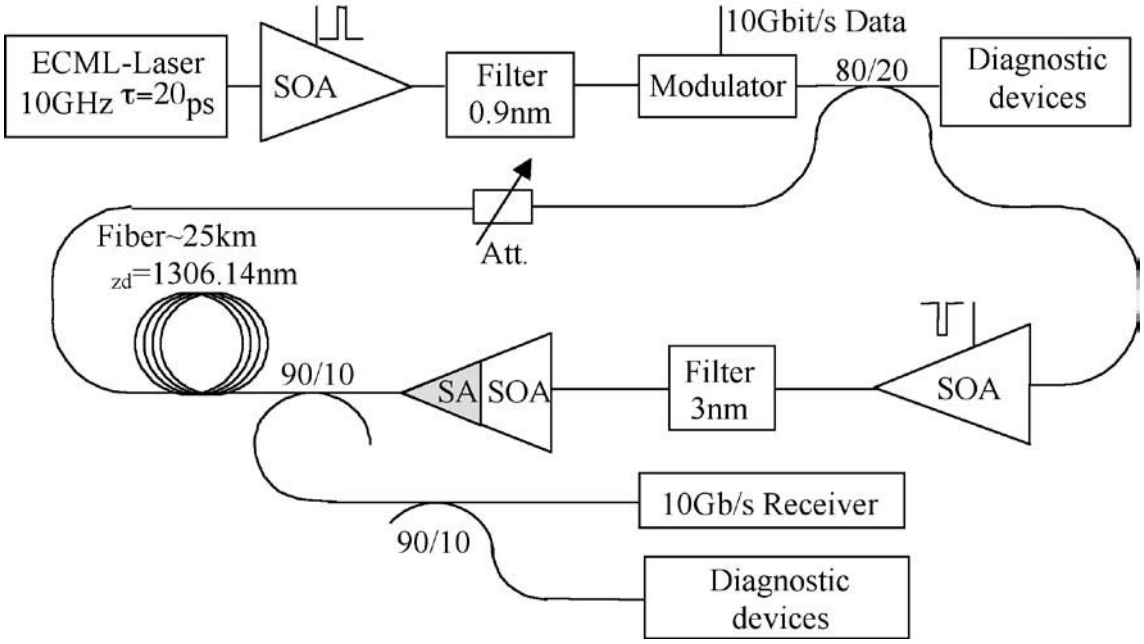

Figure 1 Re-circulating fiber loop set up for simulation of systems with in-line SOA and SA.

Semiconductor optical amplifiers (SOA) are very promising elements of integrated lightwave circuits for optical fiber communication systems. It has been previously shown by our group that Return-to-Zero (RZ) transmission in systems with in-line SOA suffers from signal decay and fast growth of amplified spontaneous emission (ASE) because of the low saturation energy and short recovery time of the SOA. It has been proposed and demonstrated that when using in-line saturable absorbers (SA), it is possible to completely suppress ASE growth and increase the maximum transmission distance many times – up to 30 000 km for 5 Gb/s using common devices. 10 Gb/s transmission over 5 000 km has been demonstrated using a gain-clamped SOA, which allows controlling of the gain recovery dynamics and minimizes the effects that limit transmission distance: bit rate dependent amplitude pattern and temporal walk off effects. These results demonstrate the world's longest transmission distances realized in the system with in-line SOA.

From a fundamental point of view, the optical fiber transmission line with in-line SOA and SA represents an essentially nonlinear, strongly dissipative system, where the parameters of the pulses (autosolitons) are completely determined by the system parameters. In contrast to conservative soliton systems, the autosoliton parameters are independent of the initial pulse parameters like duration, wavelength, and energy, and this feature has been proved in our experiments. It has been also shown that such a system with two competing noninstantaneous nonlinearities (SOA and SA) could have a new type of bifurcation behavior for a certain set of element parameters as shown in fig.2. Its specific feature is that for supercritical bifurcation of CW radiation the bifurcation of the solitons is subcritical. In the region of negative linear net gain, there are only two stable solutions – trivial zero background and autosolitons. It is in contrast to the other well known nonlinear systems with instantaneous nonlinearities where the bifurcation behavior of the CW radiation and of solitons have the same features – either both supercritical or both subcritical. Dynamics of the system have been also studied: switching of autosolitons and their relaxation. The effect of critical slowing down of the relaxation, which is typical for nonlinear systems, has been demonstrated.

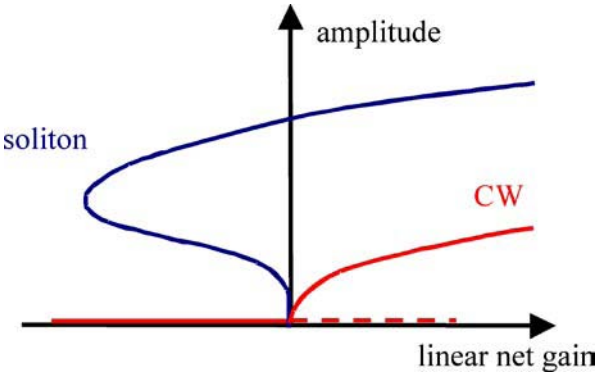

Figure 2 Bifurcation diagram of dissipative solitons in a system with competing noninstantaneous nonlinearities.

The possibility of the Non-Return-to-Zero (NRZ) transmission has been studied, too. It has been found that it is quite limited in distance – only less than ~ 1000 km are reachable because it is necessary to operate the system in a region of positive linear net gain. The transmission is limited by several instabilities of the NRZ signal. Filter bandwidth in that case plays a critical role in stabilization of signal propagation. In the case of a too broad filter – solitons are formed quickly on the leading signal edge and the top of the signal suffers from modulational instability (fig.3).

Figure 3 Results of the experiment on the decay of fronts in the case of weak filtering (3 nm),
a) 26 km **b)** 215 km **c)** 358 km (figures have different scaling).

In the case of a narrow in-line filter these instabilities are suppressed, but another effect come into play: pulse shrinkage and long soliton formation. For the first time in a dissipative optical system it has been observed that a rectangular pulse consisting of two fronts shrinks (fig.4). A formation of a long soliton with duration longer than the absorber recovery time has been demonstrated, too. Results agree well with numeral simulations.

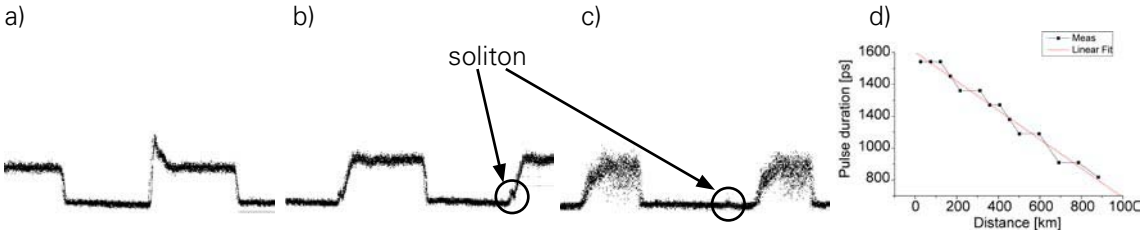

Figure 4 Results of the experiment on front dynamics in the case of strong filtering (0.2 nm),
a) 25 km **b)** 162 km **c)** 785 km
d) duration of the rectangular pulse vs. the propagation distance.

For applications timing jitter is another important parameter, which determines the transmission system performance. Investigations have shown that a very low (2 ps at 30 000 km) timing jitter could be obtained in the system (fig.5). The Gordon-Haus effect suppressed by the in-line filter has been identified as the main source of the timing jitter.

The unique features of the system with in-line SOA-SA that allow obtaining of so low jitter are the following. On the one hand, the system can operate at zero fiber dispersion with high pulse energy similar to other popular systems with dispersion management. And the energy enhancement factor is far above that of dispersion managed systems. Thus two conditions of low Gordon-Haus jitter are easy satisfied: low fiber dispersion (best system performance at zero dispersion) and high soliton energy. On the other hand, the effect of in-line SA is that a strong in-line spectral filtering can be used without transmission deterioration (growth of amplified spontaneous emission and dispersive waves). In our system the ratio of the filter bandwidth to that of the soliton could be as low as 2.

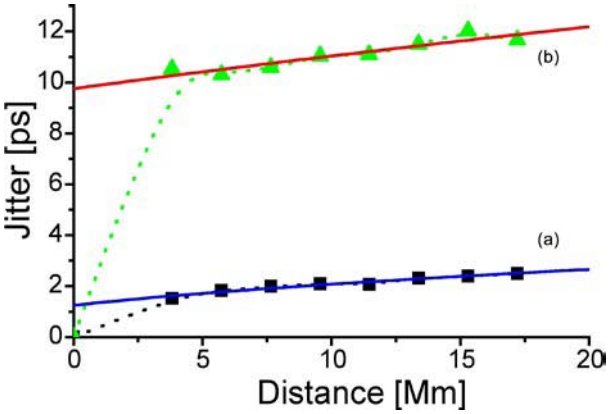

Figure 5 Distance dependence of the timing jitter for two cases: optimal (a) and bad (b) adjustment of the system. Dashed curves with points – experimental data; solid lines – fit with $\sigma_t^2 = A^2 + B^2L$. A = 1.2 ps and 9.8 ps; B = 0.5 ps/Mm$^{1/2}$ and 1.6 ps/Mm$^{1/2}$ for the two cases, accordingly.

But it has been found that in certain conditions (fig.5) the jitter accumulation during the initial transient propagation stage (first 1500 km, where the input pulses are shaped to solitons) could be very strong – about an order of magnitude large than in the optimal case. This could be harmful in practical systems with fluctuation of system parameters (mainly zero dispersion wavelength).

Most of the current systems use WDM transmission to increase the system capacity. The straightforward way of SOA-SA system extension to WDM would be demultiplexing of the channels before each amplification node and multiplexing back after it in order to avoid solitons cross talk in the main nonlinear elements of the system: SOA and SA. The possibility to use a strong in-line spectral filtering could allow to obtain improved spectral efficiency. The modernization of the experimental set up for WDM transmission and initial experiments on two-channel WDM transmission have been started.

The investigations had been partially funded by the DFG.

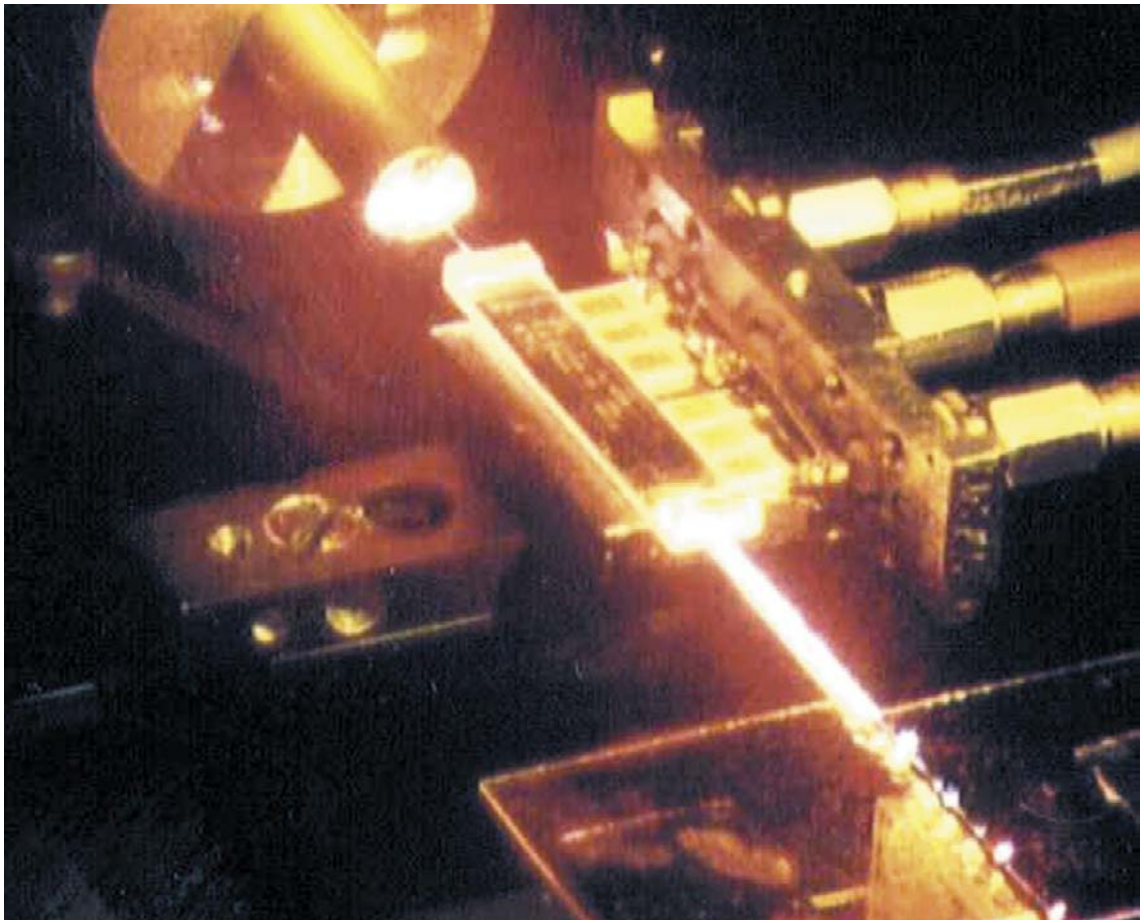

INTEGRATED OPTICS

- Epitaxial grown $K_{1-x}Rb_xTiOPO_4$ films
  with extremely flat surfaces for waveguiding

Dr. Jens-Peter Ruske

To develop integrated-optical components for compact, robust and adjustment-free systems active low-loss film and channel waveguides in sophisticated materials with high damage threshold, large electro-optical and nonlinear-optical coefficients are required. Recent work by us, dealing with optical devices in $KTiOPO_4$ [KTP] and $LiNbO_3$, confirm the superiority of KTP with regard to its greater bandwidth for ion exchanged singlemode channel waveguides and waveguide devices, smaller light-induced refractive index changes (photorefractive effect) and larger damage threshold in the visible spectral range.

Due to the inherently diffusive nature of the exchange process symmetrically waveguides, which would allow a considerably larger singlemode range and lower light scattering, cannot be realised in this way. To overcome this problem epitaxial growth techniques in combination with surface patterning techniques can be used for the fabrication of rib waveguides as well as buried waveguide structures with over-cladding layers. Among the deposition techniques the liquid phase epitaxy (LPE) is one of the most promising methods for growing µm-thick films of single-crystalline dielectric media. This method allows to prepare films of high structural perfection with extremely flat surfaces and homogeneously doped active layers, which are interesting for laser application.

We report for the first time on {100} $K_{1-x}Rb_xTiOPO_4$ films on KTP substrates grown by LPE with extremely flat surfaces that act as low-loss planar optical waveguides in the visible and near-infrared region showing transmission values comparable to conventional ion-exchanged waveguides.

Epitaxial films of {100} $K_{1-x}Rb_xTiOPO_4$ were grown by liquid phase epitaxy on commercial flux grown {100} optical-grade polished KTP substrates. Experiments were performed in the "step-cooling" mode at temperatures $T \leq 900°C$ using the vertical dipping technique under substrate rotation reversal. At supersaturations of $0 \leq \Delta T \leq 10$ K as well as cooling rates of about 1 K/hour solid-solution films of $K_{1-x}Rb_xTiOPO_4$ with $0.22 \leq x \leq 0.34$ have been obtained within 10 minutes at rotation rates of 16 rpm or without substrate rotation.

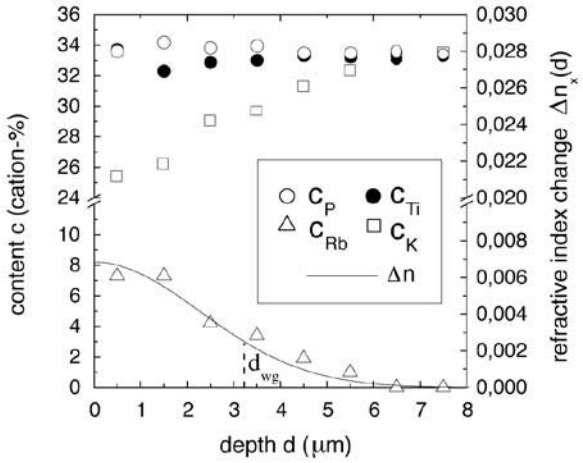

Figure 1 Concentration profiles of Rb (Δ), K (□), Ti (●) and P (○) ions and refractive index change Δn_x (TM polarisation, λ = 633 nm).

The chemical composition of the samples was analysed by energy-dispersive x-ray spectrometry (EDX) at cut and polished {010} end-faces to characterise the depth distribution of rubidium along the [100] film direction. Figure 1 presents the distribution profiles of the elements of a LPE film (related to the molar fraction of the cations in $KTiOPO_4$) with a nominal composition of $K_{0.78}Rb_{0.22}TiOPO_4$ at the film surface d = 0. Due to a non negligible Rb diffusion along the [001] KTP lattice direction the films did not show an abrupt compositional transition at the film/substrate interface.

X-ray rocking curve (XRC) analysis reveals clearly distinguished peaks for the (800) reflections of film and substrate (Fig. 2) confirming the epitaxial nature of the {h00} single-crystalline film. Spectra with full widths at half maximum (FWHM) of 36 arc-sec were obtained by high-resolution measurements. Using the lattice parameter sets of solid-solution $K_{1-x}Rb_xTiOPO_4$ members the (800) rocking curve angle separation $\Delta\theta$ between an unstrained film with $x_{surf} \approx 0.22$ and the KTP substrate is theoretically expected to be -320 arc-sec, while the experimental XRC separation angle taken from Fig. 2 is $\Delta\theta$ = -350 arc-sec. This value agrees fairly well with the calculated one suggesting an almost complete relaxation of the misfit-induced stresses due to a continuous lattice parameter distribution throughout the diffusion zone. It confirms the above given film composition measured by EDX.

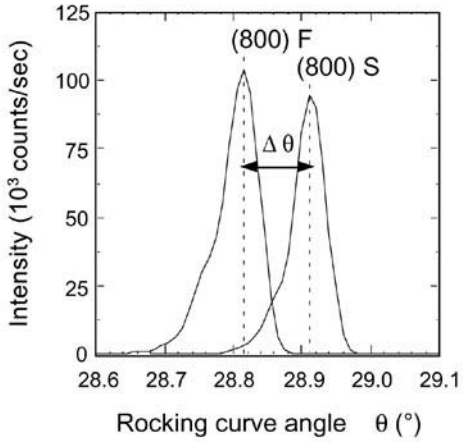

Figure 2 X-ray rocking curves of the {h00} $K_{0.78}Rb_{0.22}TiOPO_4$ film (F) and the $KTiOPO_4$ substrate (S) close to the (800) reflection for Cu K_α radiation.

Crystalline surfaces obtained by LPE can be quasi-atomically flat depending on the structural perfection and misorientation of a singular oriented substrate surface. We have prepared {100} $K_{1-x}Rb_xTiOPO_4$ films with "optically smooth" surface areas on singular {100} KTP faces. Figure 3 (a) reveals an atomic force microscopy (AFM) area scan with trains of regular step structures

parallel [010]. AFM line scans perpendicular to the observed structures (e.g. scan along A-B) reveal step heights $\Delta h < 1.3$ nm (Fig. 3(b)) which are in the order of the a-axis lattice parameter of $K_{1-x}Rb_xTiOPO_4$. The resulting rms-roughness value of ≈ 0.4 nm of this area fits the specification range of commercial available epi-polished KTP substrates.

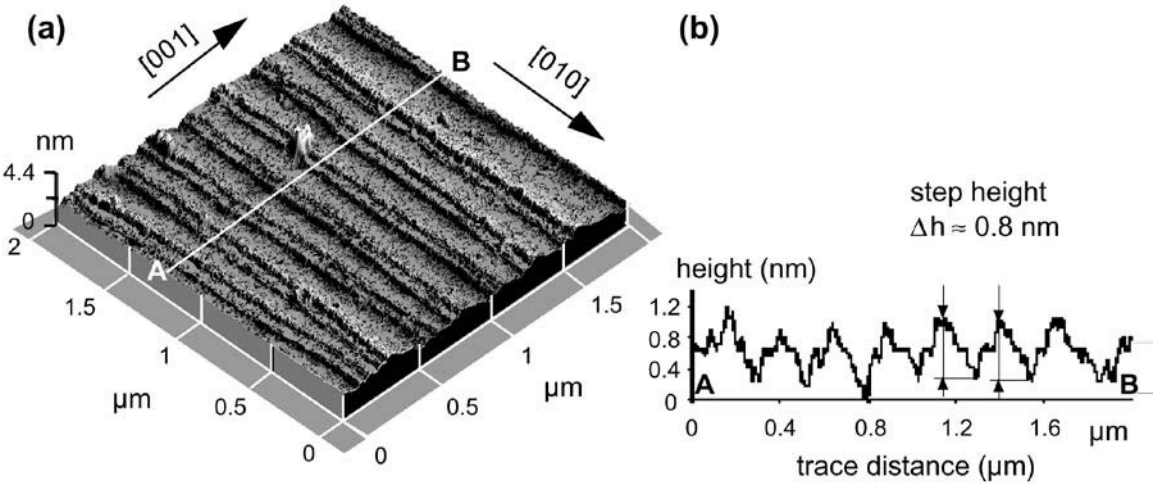

Figure 3 AFM analysis of a {100} $K_{0.78}Rb_{0.22}TiOPO_4$ film surface area.
a) area-scan **b)** line-scan perpendicular to the step structures (A–B)

The films act as multimode optical waveguides in the visible (532 nm) and singlemode in the near-infrared region (1064 nm). Using the m-line technique and assuming a Gaussian index profile a surface refractive index increase of $\Delta n_x \approx 0.007$ and a waveguide depth of d_{wg} = (3.2±0.2 µm), taken at 1/e of Δn, can be determined for the $K_{0.78}Rb_{0.22}TiOPO_4$ film for TM polarisation. For TE polarisation d_{wg} = (3.5±0.5µm) and $\Delta n_z \approx 0.004$ was measured. The obtained refractive index profile also shown in Figure 1 was found to be nearly nondispersive in the wavelength range between 476 nm and 633 nm. It corresponds fairly well with the shape of the measured rubidium distribution profile. The guided field distribution recorded by a CCD-camera is given in Fig. 4.

The optical transmission behaviour was investigated by end-face coupling of a polarised fibre input and detecting the transmitted power P_T as well as the fibre output power P_0 using a microscope objective, a slit and a large area detector. The transmission $\tau_\lambda = P_T/P_0$ was determined to be about 70% at λ = 532 nm and 65% at λ = 1064 nm for both TE and TM polarisation and a sample length of 7 mm. Taking into account the optical field overlap factor of about 0.95 and the Fresnel losses the waveguide attenuation can be calculated to be better than 1 dB/cm for TM and TE polarisation. The same values were obtained for a conventional ion-exchanged planar waveguide with the same mode behaviour.

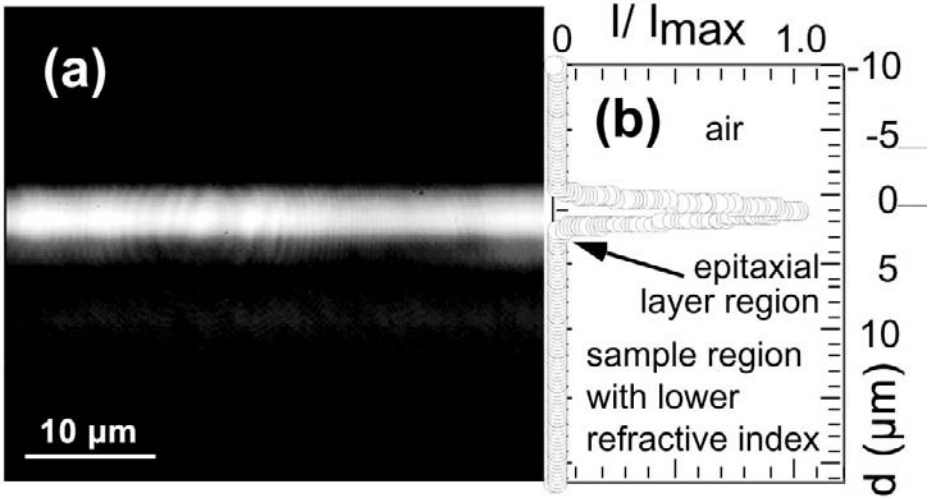

Figure 4 Near-field pattern from the {010} end-face of a planar {100} $K_{0.78}Rb_{0.22}TiOPO_4$ waveguide (fundamental mode) for TM polarisation at λ = 532 nm.

Promising results concerning the surface patterning of KTP using etching techniques have been obtained in first experiments opening up the possibility to prepare low-loss rib as well as buried channel waveguides with high-symmetrical device geometry that are compatible with fibre-optics.

Most recently, a research program on LPE-layers has been started at the institute based on this knowledge dealing with lithium-niobate as substrate material to be used in information technology.

Thanks to F. Wunderlich of the Institut für Optik and Quantenelektronik of the Friedrich-Schiller-Universität Jena for the high resolution rocking curve measurement. The financial support from the Thüringer Ministerium für Wissenschaft, Forschung und Kunst is acknowledged.

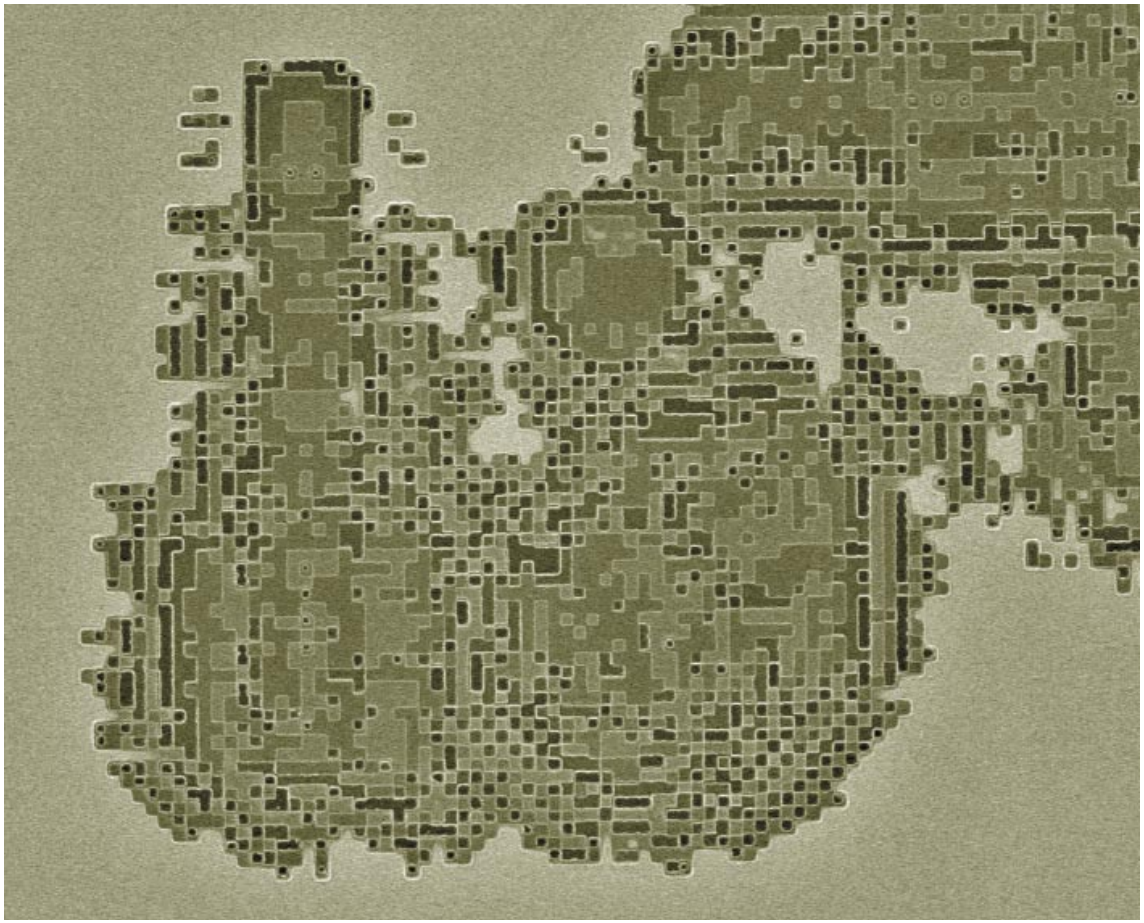

OPTICAL ENGINEERING

- Studies on Optical Vortices

Prof. Dr. Frank Wyrowski

The investigation of the wave nature of light in the design of optical systems constitutes one basic subject of the research and development of the institute. One major topic is related to the generation of special intensity distributions.

In free space, a linearly polarized monochromatic optical field

$$U = E_0 (x \pm iy)^m \exp(-ikz)$$

which satisfies the scalar wave equation, describes a single optical dislocation with topological charge given by ±m. Here E0 is a constant. The phase distribution is given by

$$\Theta(x, y) = \arg\left\{(x \pm iy)^m\right\} - kz$$

The core of the vortex has zero amplitude with undefined phase. The circulation of the gradient of the phase function around a sufficiently small positively oriented closed path C enclosing the vortex centre is 2mπ, where m is an integer denoting the topological charge

$$m = \frac{1}{2\pi} \oint_C \nabla\Theta \cdot dl$$

In Figs.1a and b the topological charge has unit magnitude. Vortices with higher magnitude of charges are uncommon. As the phase of a complex field must be single valued the topological charge of an optical vortex can take only integer values.

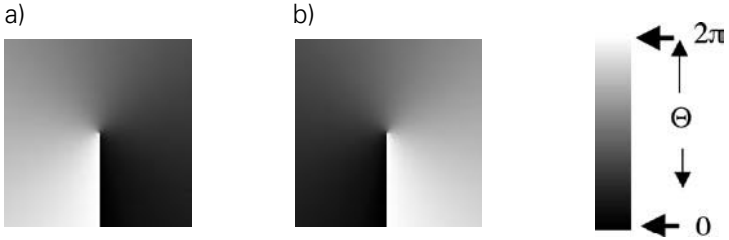

Figure 1 Phase distributions.
a) Positively charged vortex **b)** Negatively charged vortex

We have been investigating the stagnation problem caused by optical vortices in Iterative Fourier Transform Algorithms. A typical stagnated signal field distribution with large number of vortices is shown in Fig.2. This field is obtained when we try to realize band-limited complex field of an intensity object with a random phase distribution. It is closely related to the speckle problem which occurs in case of observing a random-like scattering through a finite aperture in case of coherent light.

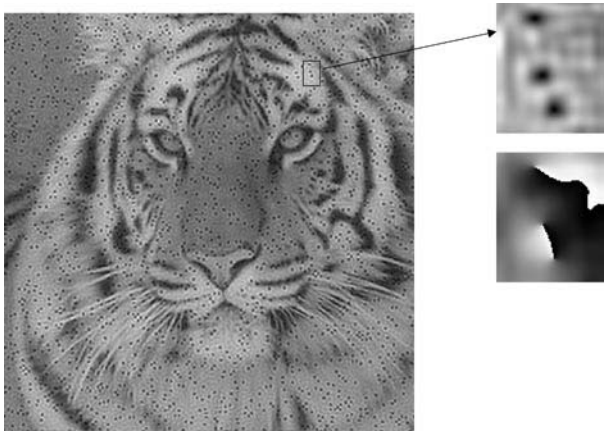

Figure 2 Stagnated signal field
Inserts – magnified view of Amplitude and Phase of vortices

Our studies identified that this stagnation problem is due to the termination of a process called self annihilation of optical vortices in the iterative algorithm. In a self annihilation process oppositely charged vortices closer to each other are mutually attracted and annihilate each other. Termination of such a process occurs when there are not enough oppositely charged vortices present in close proximity to each other. The net topological charge in any field is zero. The following figure gives the number of positively and negatively charged vortices in a random field at the end of each iteration cycle. It can be seen that the neutrality of the total charge is more or less maintained.

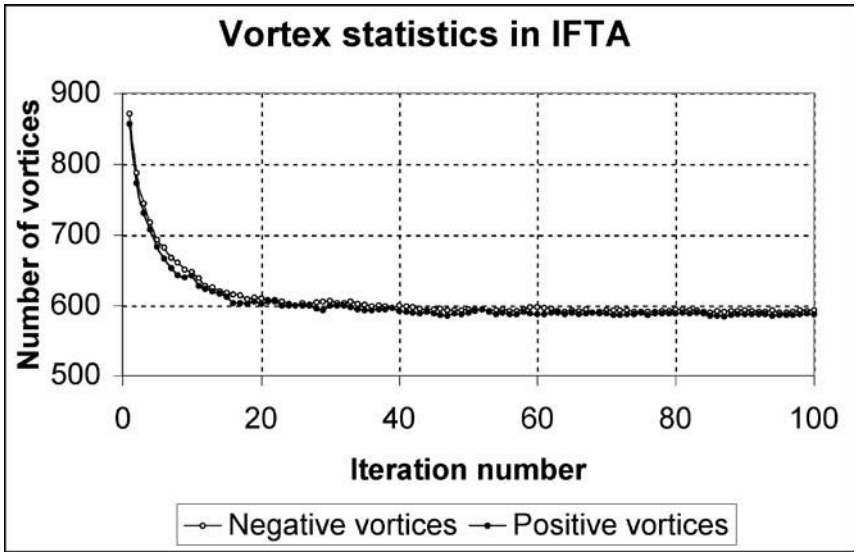

Figure 3 Vortex statistices in Iterative Fourier Transform Algorithm

At stagnation, to aid the annihilation process further, we introduce vortices in the field by identifying the charge and location of each of the vortices in the field. Again one can notice that the net charge introduced does not change the total charge in the field but will get rid of the unwanted zeros associated with optical vortices. For example, after 100 iterations, we have to

introduce roughly 1200 vortices for the case presented in Fig.3 to get vortex free signal field. The greatest advantage of this procedure lies in the realization of powerful phase synthesis algorithms in wave optical engineering as it provides a control on the appearance of vortices during iteration. Given below is the signal field obtained after the dark spots associated with the vortices are removed for the example stated earlier.

In next future, this knowledge will be used for the design of optics for real world applications.

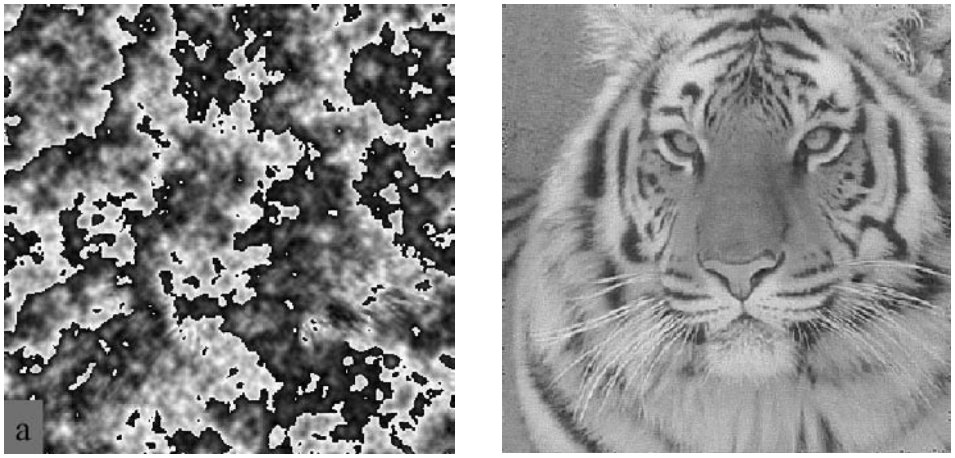

Figure 4 Phase and Amplitude distributions of the signal field.
Compare the amplitude distribution with that of Figure 2.

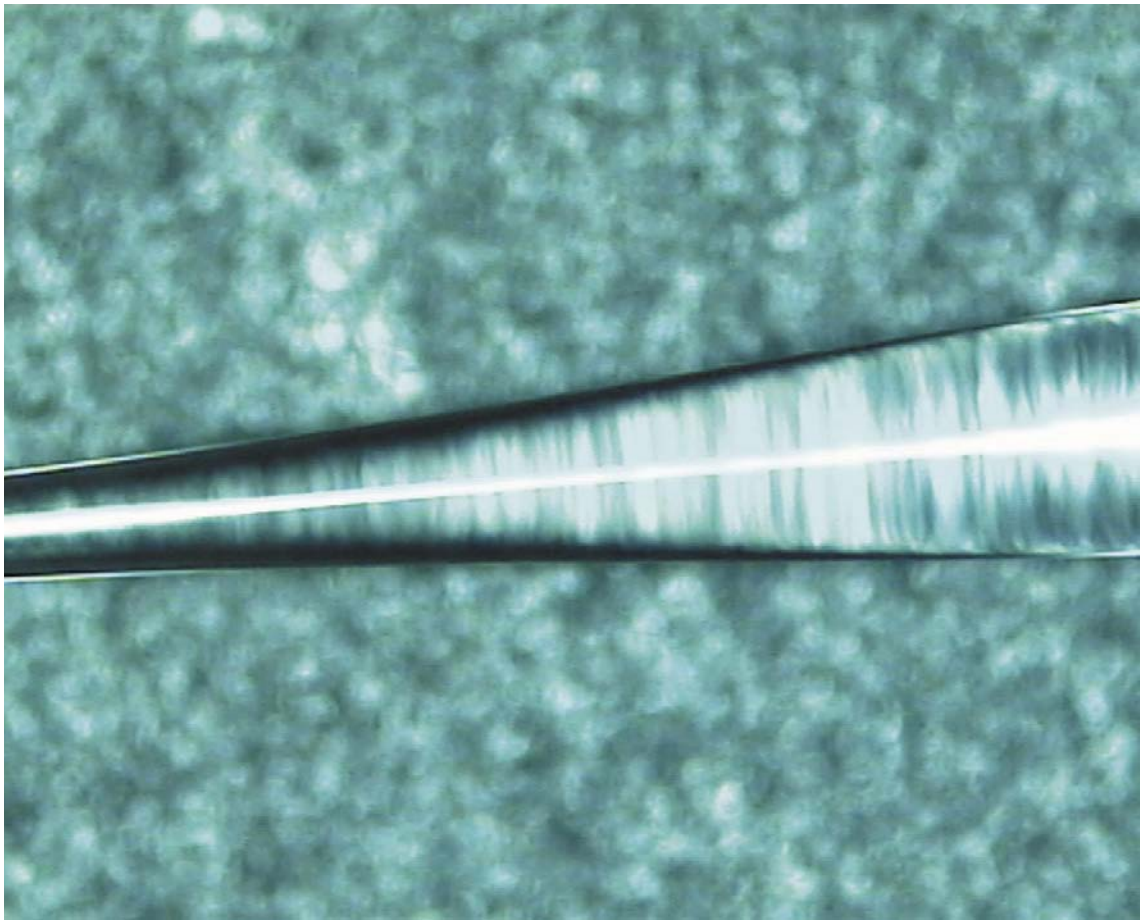

FIBER AND WAVEGUIDE LASERS

- SPM-induced spectral compression of picosecond pulses in a single-mode Yb-doped fiber amplifier

Dr. Holger Zellmer

The application of fiber and waveguide structures for the amplification of ultrashort pulses is a promising technique, which is studied at the IAP. However, self-phase modulation (SPM) usually causes spectral broadening of an ultrashort optical pulse due to the time-dependence of the nonlinear phase shift ϕ_{NL}, what is a consequence of the intensity-dependence of the refractive index. The nonlinear phase shift ϕ_{NL} is proportional to the intensity of the optical pulse and results in a frequency downshift of the leading edge and an upshift of the trailing edge of the pulse.

Depending on the initial frequency modulation (chirp) SPM leads to spectral broadening or spectral compression. Transform-limited (unchirped) or positively chirped optical pulses experience spectral broadening. In the case of negatively chirped pulses the redistribution of long and short wavelengths towards the center wavelength λ_0 results in significant spectral compression. This effect has been applied to produce transform-limited 1 ps pulses from 100 fs pulses at the end of a passively doped single-mode fiber by adapting the fiber length and the input peak power.

We report on the application of this effect in rare-earth doped fiber amplifiers to generate transform-limited high peak power picosecond pulses.

The fiber amplifier consists of a 20-m long single mode ytterbium doped fiber with a 10-µm active core and a 400-µm D-shaped pump core. We measured an M^2-value of the output of 1.1±0.1. The fiber amplifier is pumped by a pigtailed diode laser emitting up to 90 W at 915 nm.

In order to characterize the performance of the fiber amplifier, the amplification of transform-limited 10-ps pulses is studied. As 10 ps seed source a passively mode-locked Nd:YVO_4 oscillator running at 80 MHz repetition rate is applied. Seeding the fiber with 20 mW the pulses are amplified up to 6 W average power. Figure 1 shows the measured as well as the numerically simulated spectral broadening of the pulses. At an average output power of 6 W (7.5 kW peak

power) the spectrum is extended to 8.4 nm width. The inset of figure 1 shows the spectrum of the narrow-bandwidth ($\Delta\lambda$ = 0.14 nm) seed pulses and the experimentally obtained spectrum of the fiber amplified pulses at an average output power of 6 W. These results point out that the output power of conventional picosecond fiber amplifiers using standard single-mode fibers is limited to less than one watt.

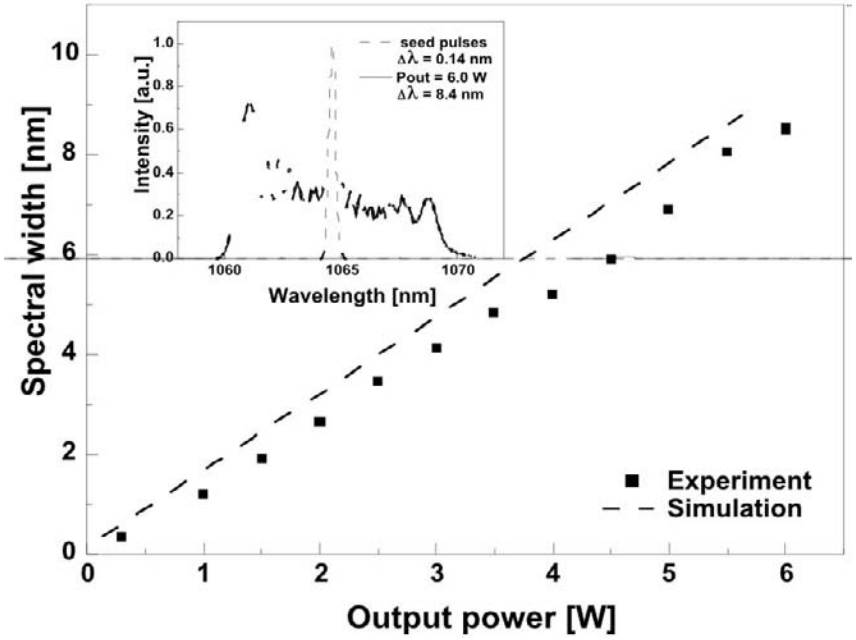

Figure 1 SPM-induced spectral broadening in a single-mode Yb-doped fiber amplifier as a function of average output power; Inset: Emitted spektrum at 6 W output power compared with the seed spectrum.

The experimental setup of our picosecond fiber amplifier using nonlinear spectral compression is shown in figure 2. The initial sech^2 pulses are generated by a passively mode-locked Nd:glass laser system. The laser is running at a repetition rate of 74 MHz, producing 150 fs pulses at a center wavelength of 1060 nm and an average power of 75 mW. The spectral width (FWHM)

of the laser is 7.8 nm, corresponding to a time-bandwidth product of 0.312. A bulk Faraday isolator protects the oscillator from back reflections. The negative chirp is created by a pair of 1200-lines/mm gold coated diffraction gratings (1000-nm blaze wavelength) with a compact size of 2.5 x 2.5 cm. The gratings were used at an angle of diffraction of 30.5°, i.e. 9° off-Littrow's mounting.

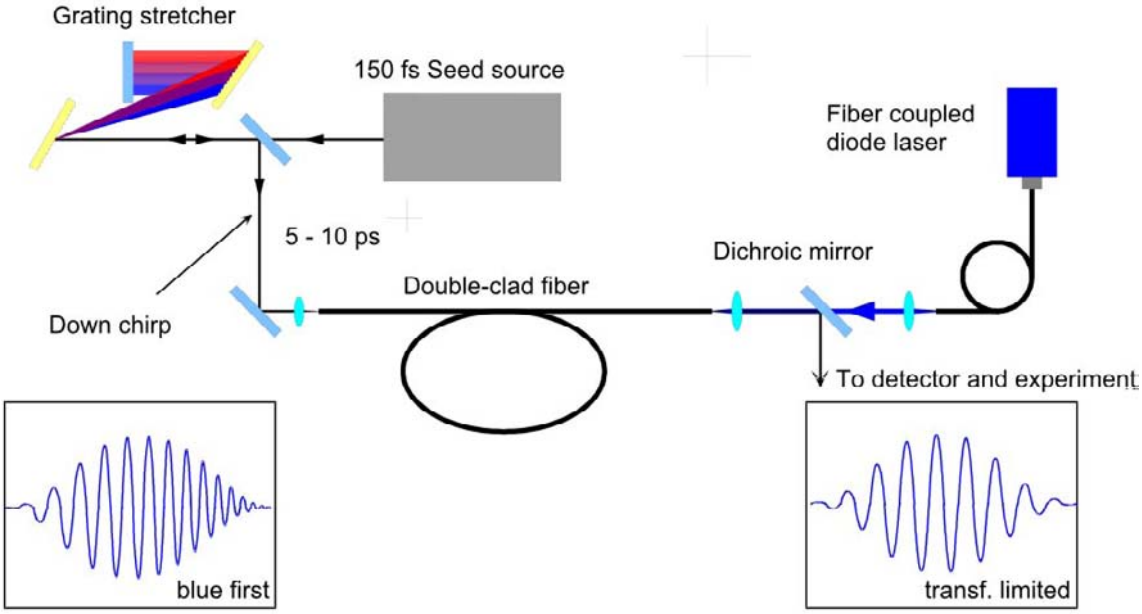

Figure 2 Experimental setup of the high peak power fiber amplifier

Two different stretcher configurations are used to demonstrate the effect of spectral compression in fiber amplifiers. At a grating separation of 12.5 cm the 150 fs pulses are negatively chirped and stretched to about 13 ps pulse duration. The efficiency of the grating stretcher in a double pass is 50%, therefore about 20 mW average power of negatively chirped picosecond pulses are launched in the active core of the fiber amplifier. Figure 3 shows the spectral compression of the pulses as a function of the average output power.

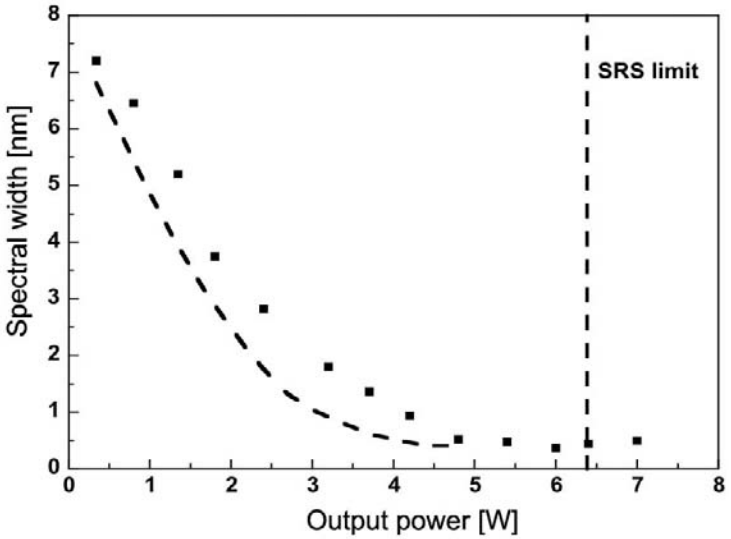

Figure 3 Development of the spectral width versus the average output power in the case of 12.5 cm grating separation.
Dashed curve: Numerical simulations

At an output power of 6 W the spectral width is reduced to 0.37 nm, corresponding to a compression ratio of 21. The nonlinear Schrödinger equation describes the propagation of short optical pulses through single-mode fibers, which can be solved using the split-step Fourier method. The dashed curve in figure 3 represents numerical simulations of the propagation of the pulses, which experience gain, group-velocity dispersion and optical nonlinearity in the amplifier fiber. The comparison of the simulated and measured spectra in figure 3 shows a good agreement. The slight deviation has the origin in the simplifying assumption of an exponentially growing pulse peak power in the fiber amplifier. At an average output power of 6.3 W we observed a signal at 1120 nm about 40 dB below the pulse at 1060 nm indicating SRS. The SRS threshold is marked in figure 3 by a vertical dashed line. The measured spectra at different output powers and the spectrum of the Nd:glass oscillator are shown in figure 4.

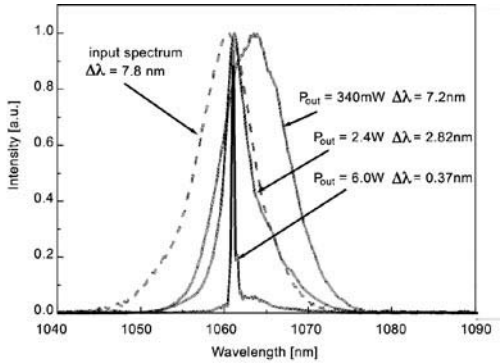

Figure 4 Solid lines: Emitted spectra at different output powers (12.5 cm grating separation)
Dashed line: Spectrum of the Nd:glass laser

The redshift of the amplified pulses is due to the misfit between the input spectrum and the gain distribution of this ytterbium-doped fiber amplifier. Nevertheless, the spectrum of the pulses compresses near the center wavelength of 1060 nm. Figure 5 shows the intensity autocorrelation trace determined by non-collinear second-harmonic generation of the pulses at the maximal spectral compression point.

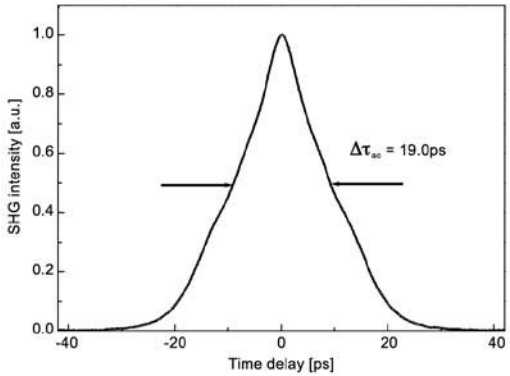

Figure 5 Intensity autocorrelation trace of the emitted pulses at the maximum spectral compression point in the case of 12.5 cm grating separation.

The emitted pulses have an autocorrelation width of 19 ps. However, the measured autocorrelation trace shows an undefined shape and the reconstruction of the actual shape of the pulses would be possible only using a FROG-measurement. A straightforward calculation of the evolution of the negatively chirped pulses in the normal-dispersion regime of the 20-m long fiber amplifier reveals that the pulse duration (FWHM) is reduced to about 11.5 ps at the point of narrowest spectral width. This would correspond to a peak power in the range of 7 kW and a time-bandwidth product of about 1.1.

At a grating separation of 7.0 cm the pulses of the femtosecond oscillator are stretched to about 7.0 ps pulse duration. At an average output power of 2.3 W the spectral width is reduced to 0.48 nm, according to a compression ratio of about 16. The autocorrelation trace of the pulses at the 2.3 W average output power shows a width of 9.0 ps with a shape similar to the trace shown in figure 5. Based on the same considerations as done in the longer pulse case the pulse duration (FWHM) can be estimated to 6.0 ps, corresponding to a time bandwidth product of 0.77. The reached peak power at this shorter pulse duration is about 5.2 kW.

One benefit of the method is that a variation of the pulse duration is simply done by changing the grating separation. The lower limit of pulse duration is given by the fact that the negative chirp which is imposed to the pulses before the amplification should be significantly larger than the positive chirp of the dispersive fiber. High power rare-earth-doped fiber amplifiers with only few meters of fiber length are demonstrated, therefore even pulse durations shorter than 1 ps are possible using the SPM-induced spectral compression method. There is no upper limit of achievable pulse duration. A fundamental limit of producible pulse peak power sets the Raman threshold.

Basically, the achievable pulse peak power at the maximal spectral compression point is determined by the fiber design, i.e. the core diameter and the fiber length. Actively doped fibers with core diameters of several 10 µm and diffraction limited output are demonstrated. Therefore, transform-limited picosecond pulses with peak powers up to 100 kW seem to be feasible in such a fiber amplifier system, what makes this laser suitable as compact pump source for

frequency upconversion using narrow-bandwidth nonlinear crystals. Furthermore, the complexity of the system can be significantly reduced by the use of a chirped fiber bragg grating or a photonic band gap fiber instead of the bulk grating stretcher to provide anomalous group-velocity dispersion.

In conclusion, we have demonstrated a scalable fiber based approach of high peak power picosecond pulse generation with adjustable pulse duration. We reached pulse peak powers of up to 7 kW out of a single-mode fiber amplifier. A good agreement between the experimentally observed and numerically simulated output spectra is shown. The presented laser concept has the potential to realize a compact high peak power near-transform limited short pulse source. Investigations on power scaling are presently under progress.

The investigations had been partially funded by the BMBF.

Journals

C. Bauer, H. W. Giessen, **B. Schnabel, E.-B. Kley**, C. Schmitt, U. Scherf, R. F. Mahrt: Circular dielectric gratings acting as resonators for solid state polymer, Proc. SPIE 4440, 194–201 (2001)

M. Cumme, H. Hartung, L. Wittig, E.-B. Kley: Thick refractive beam shaping elements applied to laser diodes; Proc. SPIE 4440, 25–33 (2001)

C. Dubs, J.-P. Ruske, E. Werner, A. Tünnermann, Ch. Schmidt, G. Bruchlos: Epitaxial grown $K_{1-x}Rb_xTiOPO_4$ films with extremely flat surfaces for waveguiding; Optical Materials 17, 477–481 (2001)

S. Höfer, A. Liem, J. Limpert, H. Zellmer, A. Tünnermann, S. Unger, S. Jetschke, H.-R. Müller, I. Freitag: Single-frequency master-oscillator fiber power amplifier system emitting 20 W of power; Optics Letters 26, 1326–1328 (2001)

E.-B. Kley, W. Rockstroh, H. Schmidt, A. Drauschke, F. Wyrowski: Investigation of large null-CGH realization; Proc. SPIE 4440, 135–144 (2001)

E.-B. Kley, H. Fuchs, A. Kilian: Fabrication of glass lenses by melting technology; Proc. SPIE 4440, 85–92 (2001)

C.Knöll, M.Gölles, **Z.Bakonyi, G.Onishchukov**, F.Lederer: Optimization of signal transmission by in-line semiconductor optical amplifier-saturable absorber module; Optics Communications 187, 141–153 (2001)

F. Korte, **S. Nolte**, B. N. Chichkov, C. Fallnich, **A. Tünnermann**, H. Welling: Submicron structuring of solid targets with femtosecond laser pulses, Proc. SPIE 4274, 110–115 (2001)

A. Liem, J. Limpert, H. Zellmer, A. Tünnermann, D. Nickel, U. Griebner, G. Korn, S. Unger: High energy ultrafast fiber CPA system; TOPs 50, 111–113 (2001)

J. Limpert, T. Gabler, **A. Liem, H. Zellmer, A. Tünnermann**: SPM-induced spectral compression of picosecond pulses in a single-mode Ytterbium-doped fiber amplifier; Applied Physics B 74, 191–195 (2001)

J. Limpert, A. Liem, T. Gabler, **H. Zellmer, A. Tünnermann**, S. Unger, S. Jetschke, H.-R. Müller: High-average-power picosecond Yb-doped fiber amplifier; Optics Letters 26, 1849 (2001)

J. Limpert, A. Liem, S. Höfer, T. Gabler, **H. Zellmer, A. Tünnermann**, S. Unger, S. Jetschke, H.-R-Müller: High avarage power ultrafast Yb-doped fiber amplifier; TOPs 50, 348–354 (2001)

J. Limpert, H. Zellmer, P. Riedel, A. Tünnermann: Investigations on novel upconversion processses in rare earth doped fluorozirconate glass; TOPs 50, 270–272 (2001)

D. Nickel, **A. Liem, J. Limpert, H. Zellmer**, U. Griebner, S. Unger, G. Korn, **A. Tünnermann**: Fiber based high repetition rate, high energy laser source applying chirped pulse amplification; Optics Communications 190, 309–315 (2001)

S. Nolte, M. Will, M. Augustin, P. Triebel, K. Zöllner, A. Tünnermann: Cutting of optical materials by using femtosecond laser pulses; Proc. SPIE 4440, 152–160 (2001)

A.G.Okhrimchuk, **G.Onishchukov**, F.Lederer: Long-haul soliton transmission at 1.3 µm using distributed Raman amplification; IEEE/OSA Journal of Lightwave Technology 19, 837–841 (2001)

A. Tünnermann, H. Zellmer: Faserlaser – Grundlagen und Anwendungen; Laser Magazin 2, 12 (2001)

L.-C. Wittig, M. Cumme, S. Nolte, E.-B. Kley, A. Tünnermann: Beam shaping for multimode beams; Proc. SPIE 4440, 34–39 (2001)

Conference Contributions

Z.Bakonyi, D.Michaelis, U.Peschel, **G.Onishchukov**, C.Knöll, F.Lederer: Stable dissipative solitons with competing non-instantaneous nonlinearities, Nonlinear Guided Waves and Their Applications (NLGW'2001); Clearwater, Florida, USA, Technical Digest, paper MC72, pp. 251–253 (2001)

Z.Bakonyi, G.Onishchukov, C.Knöll, D.Michaelis, U.Peschel, F.Lederer: Timing jitter in autosoliton fiber communication systems with semiconductor optical amplifiers and saturable absorbers, 10th European Conference on Integrated Optics (ECIO'2001); Paderborn, Germany, Technical Digest, paper FrB1.5, pp. 407–410 (2001)

Z.Bakonyi, G.Onishchukov, U.Peschel, C.Knöll, D.Michaelis, F.Lederer: Timing jitter in system with semiconductor optical amplifiers and saturable absorbers, COST 267 / SCOOP International Workshop on Optical Signal Processing; Lyngby, Denmark, November 29–30 (2001)

C. Bauer, H. Giessen, **B. Schnabel, E.-B. Kley**, U. Scherf, C. Schmitt, R. F. Mahrt: A novel optically pumped polymer laser based on a circular grating structure; SYOF, DPG 2001

T. Gorelik, **M. Will, A. Tünnermann**, U. Glatzel: A Transmission Electron Microscopy (TEM) Study of Femtosecond Laser Included Modifications in Quartz; Spring Meeting of the Materials Research Society, San Francisco, USA (2001)

S. Höfer, J. Limpert, H. Zellmer, A. Tünnermann, S. Unger, S. Jetschke, H.-R. Müller: Single frequency master-oscillator fiber power amplifier system with 20 W output power; CLEO/Europe-EQEC Focus Meeting: Progress in Solid State Lasers, Munich 2001

S. Höfer, H. Zellmer, A. Tünnermann, S. Unger, S. Jetschke, H.-R. Müller: High power single frequency master-oscillator fiber amplifier system; DPG Spring Meeting, Berlin, April 2–6, 2001, Paper Q 31.9 (2001)

C.Knöll, D.Michaelis, **Z.Bakonyi**, U.Peschel, **G.Onishchukov**, F.Lederer: Signal stability in transmission lines with semiconductor optical amplifier and saturable absorption, COST 267 / SCOOP International Workshop on Optical Signal Processing; Lyngby, Denmark, November 29–30 (2001)

F. Korte, **S. Nolte**, B.N. Chichkov, C. Fallnich, **A. Tünnermann**, H. Welling: Submicron structuring of solid targets with femtosecond laser pulses; SPIE Photonics West 2001, San Jose, USA

A. Liem, J. Limpert, T. Gabler, **H. Zellmer, A. Tünnermann**, S. Unger, S. Jetschke, H.-R. Müller: 50 W avarage power ultrafast Yb-doped fiber amplifier; DPG Spring Meeting, Berlin, April 2–6, 2001, Paper Q 33.2 (2001)

A. Liem, J. Limpert, T. Schreiber, S. Nolte, H. Zellmer, A. Tünnermann: High average power femtosecond fiber CPA system; Norddeutscher Lasertag, Hamburg, December 5, 2001

A. Liem, J. Limpert, H. Zellmer, A. Tünnermann, D. Nickel, U. Griebner, G. Korn, S. Unger, S. Jetschke, H.-R. Müller: Ultrafast fiber CPA system; CLEO/Europe-EQEC Focus Meeting: Progress in Solid State Lasers, Munich 2001

A. Liem J. Limpert, H. Zellmer, A. Tünnermann, D. Nickel, U. Griebner, G. Korn, S. Unger: High energy ultrafast fiber CPA system; Advanced solid state lasers, paper MB-13 (2001)

A. Liem, H. Zellmer, J. Limpert, P. Riedel, A. Tünnermann: 25 W all fiber pump source at 1120 nm; Conference on Lasers and Electro-Optics CLEO, May 6–11, 2001, Baltimore, USA, P. CTuQ1

J. Limpert, A. Liem, H. Zellmer, A. Tünnermann, T. Gabler: High avarage power ultrafast Yb-doped fiber amplifier; Advanced solid state lasers, paper TuA2 (2001)

J. Limpert, A. Liem, H. Zellmer, A. Tünnermann, D. Nickel: Ultrafast fiber CPA system; DPG Spring Meeting, Berlin, April 2–6, 2001, Paper Q 33.3 (2001)

J. Limpert, H. Zellmer, A. Liem, P. Riedel, A. Tünnermann: Laser oscillation in the yellow and blue spectral range in Dy^{3+}:ZBLAN; Conference on Lasers and Electro-Optics CLEO, May 6–11, 2001, Baltimore, USA , P. CWJ4

J. Limpert, H. Zellmer, P. Riedel, A. Tünnermann: Investigations on novel upconversion processes in rare earth doped fluorozirconate glass; Advanced solid state lasers, paper ME13 (2001)

D.Michaelis, **Z.Bakonyi**, U.Peschel, **G.Onishchukov**, F.Lederer: Dissipative solitons in fiber transmission lines with semiconductor optical amplifiers, 10th European Conference on Integrated Optics (ECIO'2001); Paderborn, Germany, Technical Digest, paper FrB1.6, pp. 411–414 (2001)

D.Michaelis, **Z.Bakonyi**, U.Peschel, **G.Onishchukov**, F.Lederer: Anomalous front dynamics in dissipative systems, Nonlinear Guided Waves and Their Applications (NLGW'2001); Clearwater, Florida, USA, Technical Digest, paper TuA7, pp. 361–363 (2001)

D. Nickel, U. Griebner, G.Korn, **A. Liem, J. Limpert, H. Zellmer, A. Tünnermann**: Fiber based chirped pulse amplification system with 22 W output power; Conference on Lasers and Electro-Optics CLEO, May 6–11, 2001, Baltimore, USA , P. CMA6

S. Nolte, M. Will, M. Augustin, P. Triebel, A. Tünnermann, T. Gorelik, F.Wunderlich: Fabrication of optical waveguides inside transparent materials using ultrashort laser pulses; Nonlinear Guided Waves and Their Applications, Clearwater, USA (2001)

S. Nolte, M. Will, M. Augustin, B.N. Chichkov, **K. Zöllner, A. Tünnermann**: Cutting of optical materials by using femtosecond laser pulses; SPIE Annual Meeting 2001, San Diego, USA

S. Nolte, M. Will, M. Cumme, B.N. Chichkov, **A. Tünnermann**, F. Korte, A. Egbert: Sub-micrometer structuring of metals with femtosecond laser pulses; CLEO 2001, Baltimore, USA

A. Tünnermann: Faserlaser – Grundlagen und Anwendungen; DPG-Kolloquium, Aalen (2001); invited

A. Tünnermann: Faserlaser und –verstärker hoher Leistung im kontinuierlichen und gepulsten Betrieb; PTB-Kolloquium, Braunschweig (2001); invited

A. Tünnermann: Mikro- und Nanooptik; Physikalisches Kolloquium der Universität Rostock (2001); invited

A. Tünnermann: Micro- and Nano-Optics; ZEMO-Optik-Symposium, Friedrich-Alexander-Universität Erlangen-Nürnberg (2001); invited

A. Tünnermann: Grundlagen von Hochleistungsfaserlasern und –verstärkern; Physikalisches Kolloquium der TU-Ilmenau (2001); invited

A. Tünnermann, E.-B. Kley: Micro- and nano-structured optics; Norddeutscher Lasertag, Hamburg (2001); invited

A. Tünnermann: High power fiber and waveguide lasers; Symposium on Advanced Photon Research, JAERI Nara, Japan (2001); invited

A. Tünnermann: Optical Technologies Made in Germany; Symposium on Advanced Photon Research, JAERI Nara, Japan (2001); invited

E.A. Werner, J.-P. Ruske, B. Zeitner, W. Biehlig, **A. Tünnermann**: Integrated-optical high power amplitude modulator for the visible wavelength range in KTP; Proc. European Conference on Integrated Optics (ECIO´01), April 4–6, 2001, Paderborn, pp. 168–171

M. Will, A. Tünnermann, S. Nolte, F. Wunderlich, K. Goetz, T. Gorelik, U. Glatzel: Properties of waveguides produced with ultrashort laser pulses; Frühjahrstagung der DPG 2001, Berlin

M. Will, S. Nolte, J.-P. Ruske, F. Wunderlich, **A. Tünnermann**: Properties of waveguides manufactured with fs-laser pulses in transparent materials; CLEO 2001, Baltimore, USA

L.-C. Wittig, M. Cumme, S. Nolte, E.-B. Kley, A. Tünnermann: Beam shaping for multimode beams; SPIE Annual Meeting 2001, San Diego, USA

H. Zellmer, S. Höfer, A. Liem, J. Limpert, P. Riedel, A. Tünnermann: Fiber amplifiers for ultrashort pulses (invited); German-Israeli Workshop 2001 "Solid State Lasers", Stade, October 22–24, 2001

H. Zellmer, P. Riedel, A. Tünnermann: High power multi mode visible upconversion fiber laser in the red spectral range; CLEO/Europe-EQEC Focus Meeting: Progress in Solid State Lasers, Munich 2001

Patent Applications

H.Zellmer, G.Henning: Anordnung zur schnellen elektro-optischen Amplituden- oder Phasen-Modulation von polarisiertem Laserlicht; Patent Nr. 101 42 255,5; Applicant: Schepers Ohio GmbH

Fairs

Campus-Präsentation, Jena	Presentation of laser printing
LASER 2001, München	Presentation of fiber lasers and integrated-optical modulators
ECIO 01 Paderborn (April 2001)	Presentation of integrated-optical modulators

Organizing Activities

Prof. Dr. Andreas Tünnermann

ASSL 2001 (Seattle)	Program Committee Member
CLEO/EUROPE Focus Meeting (München)	General Program Chair Solid State Lasers
Beutenberg Campus e.V.	Founder and Member
BMBF-Fact Finding Mission Canada	Member
BMBF-Leitprojekt „MIKROPHOT"	Network Coordinator
Forschungsschwerpunkt Optomatronik/ Zentrum für Optomatronik	Founder and Member of the Board
Guided Color Technologies GmbH	Partner
Kompetenzzentrum UPOB	Member
Laser Zentrum Hannover e.V.	Member
OptoNet e.V.	Founder and Member of the Board
Wissenschaftliche Gesellschaft Lasertechnik e.V.	Member

Dr. Stefan Nolte

CLEO 2001 (Baltimore, Maryland/USA)	Program Committee Member "Laser Applications and Optical Instrumentation Systems"

Dr. Ernst-Bernhard Kley

Lithographic and Micromachining Techniques for Optical Component Fabrication	Conference Chair
Dr. Holger Zellmer	
CLEO 2001 (Baltimore, Maryland/USA)	Program Committee Member

Postal address

Friedrich-Schiller-Universität Jena
Institut für Angewandte Physik
Max-Wien-Platz 1
D-07743 Jena, Germany

Location of the institute

Beutenberg Campus
Winzerlaer Straße 10
D-07745 Jena

Phone +49 (0) 36 41. 65 76 40
Fax +49 (0) 36 41. 65 76 80
Internet http://www.iap.uni-jena.de

Director of the institute
Prof. Dr. Andreas Tünnermann
Phone +49 (0) 36 41. 65 76 46
e-mail tuennermann@iap.uni-jena.de

Optical Engineering
Prof. Dr. Frank Wyrowski
Phone +49 (0) 36 41. 65 76 64
e-mail wyrowski@uni-jena.de

Microstructure Technology · Microoptics
Dr. Ernst-Bernhard Kley
Phone +49 (0) 36 41. 65 76 47
e-mail kley@iap.uni-jena.de

Ultrafast Optics
Dr. Stefan Nolte
Phone +49 (0) 36 41. 65 76 56
e-mail nolte@iap.uni-jena.de

Optical Communication Systems
Dr. George Onishchukov
Phone +49 (0) 36 41. 65 76 60
e-mail george.onishchukov@uni-jena.de

Integrated Optics
Dr. Jens-Peter Ruske
Phone +49 (0) 36 41. 65 76 45
e-mail ruske@iap.uni-jena.de

Fiber and Waveguide Lasers
Dr. Holger Zellmer
Phone +49 (0) 36 41. 65 76 51
e-mail zellmer@iap.uni-jena.de

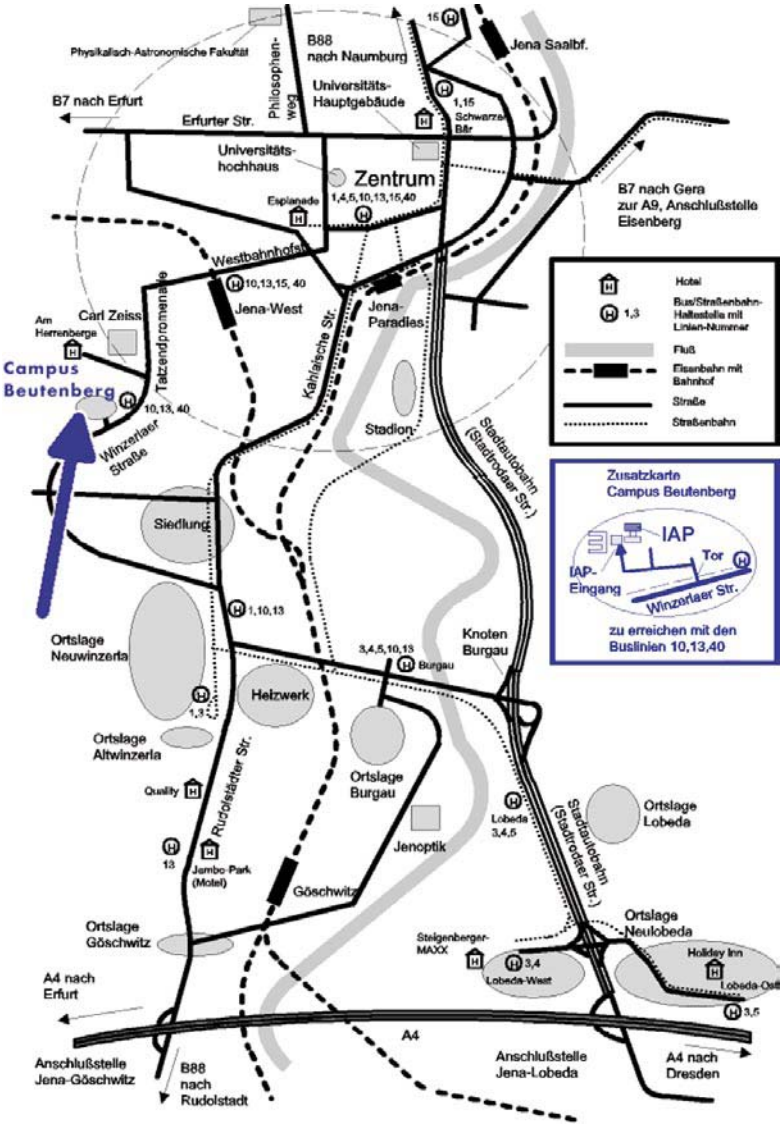
Physikalisch-Astronomische Fakultät
B88
nach Naumburg
Philosophen-
weg
Universitäts-
Hauptgebäude
15
Jena Saalbf.
1,15
Schwarze
Bär
B7 nach Erfurt
Erfurter Str.
Universitäts-
hochhaus
Zentrum
1,4,5,10,13,15,40
Esplanade
B7 nach Gera
zur A9, Anschlußstelle
Eisenberg
Westbahnhof
10,13,15, 40
Jena-West
Jena-
Paradies
Kahlaische Str.
Am
Herrenberge
Carl Zeiss
Campus
Beutenberg
Tatzendpromenade
10,13, 40
Winzerlaer
Straße
Stadion
Stadtautobahn
(Stadtrodaer Str.)
Siedlung
1,10,13
Ortslage
Neuwinzerla
3,4,5,10,13
Burgau
Knoten
Burgau
Heizwerk
1,3
Ortslage
Altwinzerla
Quality
Rudolstädter Str.
Ortslage
Burgau
Lobeda
3,4,5
Ortslage
Lobeda
Stadtautobahn
(Stadtrodaer Str.)
13
Jambo-Park
(Motel)
Jenoptik
Göschwitz
Ortslage
Göschwitz
Steigenberger-
MAXX
Ortslage
Neulobeda
Holiday Inn
Lobeda-Ost
3,4
Lobeda-West
3,5
A4 nach
Erfurt
A4
Anschlußstelle
Jena-Göschwitz
B88
nach
Rudolstadt
Anschlußstelle
Jena-Lobeda
A4 nach
Dresden
Hotel
1,3
Bus/Straßenbahn-
Haltestelle mit
Linien-Nummer
Fluß
Eisenbahn mit
Bahnhof
Straße
Straßenbahn
Zusatzkarte
Campus Beutenberg
IAP
Tor
IAP-
Eingang
Winzerlaer Str.
zu erreichen mit den
Buslinien 10,13,40